Published in final edited form as:
Traffic. 2013 March ; 14(3): 337–354. doi:10.1111/tra.12032.

Basolateral EGF receptor sorting regulated by functionally distinct mechanisms in renal epithelial cells

Calvin U. Cotton[1,2], **Michael E. Hobert**[2], **Sean Ryan**[3,†], and **Cathleen R. Carlin**[2,3,4,‡]

[1]Department of Pediatrics, School of Medicine, Case Western Reserve University, Cleveland, Ohio 44106-4970

[2]Department of Physiology and Biophysics, School of Medicine, Case Western Reserve University, Cleveland, Ohio 44106-4970

[3]Department of Molecular Biology and Microbiology, School of Medicine, Case Western Reserve University, Cleveland, Ohio 44106-4970

[4]Case Western Reserve University Comprehensive Cancer Center, School of Medicine, Case Western Reserve University, Cleveland, Ohio 44106-4970

Abstract

Proliferation of epithelial tissues is controlled by polarized distribution of signaling receptors including the EGF receptor (EGFR). In kidney, EGFRs are segregated from soluble ligands present in apical fluid of nephrons by selective targeting to basolateral membranes. We have shown previously that the epithelial-specific clathrin adaptor AP1B mediates basolateral EGFR sorting in established epithelia. Here we show that protein kinase C (PKC)-dependent phosphorylation of Thr654 regulates EGFR polarity as epithelial cells form new cell-cell junctional complexes. The AP1B-dependent pathway does not override a PKC-resistant T654A mutation, and conversely AP1B-defective EGFRs sort basolaterally by a PKC-dependent mechanism, in polarizing cells. Surprisingly, EGFR mutations that interfere with these different sorting pathways also produce very distinct phenotypes in three-dimensional organotypic cultures. Thus EGFRs execute different functions depending on the basolateral sorting route. Many renal disorders have defects in cell polarity and the notion that apically mislocalized EGFRs promote proliferation is still an attractive model to explain many aspects of polycystic kidney disease. Our data suggest EGFR also integrates various aspects of polarity by switching between different BL sorting programs in developing epithelial cells. Fundamental knowledge of basic mechanisms governing EGFR sorting therefore provides new insights into pathogenesis and advances drug discovery for these renal disorders.

Keywords

EGF receptor; membrane trafficking; protein kinase C; renal epithelial cells; sorting signal

[‡]**Corresponding author:** Cathleen Carlin, Department of Molecular Biology and Microbiology, School of Medicine, 10900 Euclid Avenue, Cleveland, Ohio, 44106-4920, Telephone (216) 368-8939, Telefax 216-368-3055, cathleen.carlin@case.edu.
[†]**Current address:** Department of Cell Biology, Duke University Medical Center, Durham, NC 27710

Introduction

The kidney regulates salt and water balance, blood pressure, pH, and nitrogenous waste to maintain constancy of the internal environment (1). The nephron is the kidne's main functional unit. Fluid forced out of the blood through capillary walls of the glomerulus flows into an adjacent renal tubule and collecting duct (CD) system where urine is produced and concentrated (1). Tubules and CD are lined by polarized epithelial cells that facilitate specialized reabsorption and secretion functions along the length of the nephron (2). Acute renal failure, chronic kidney disease, and juvenile and adult forms of polycystic diseases (PKD) that collectively afflict more than 10% of the US adult population are often accompanied by pathological defects in epithelial cell polarity (3). Cysts that obstruct normal kidney function expand because epithelial cells lining the cyst hyper-proliferate, yet PKD patients do not have an increased risk to develop cancer (4). Cystic cells therefore offer a unique vantage point to characterize cell polarity changes along a pathological continuum that falls short of cell transformation. Thus, understanding the molecular mechanisms that lead to the loss of epithelial cell polarity has broad clinical relevance.

Epithelial cells exhibit two forms of cell polarity. Apical-basolateral (Ap-BL) polarity refers to the asymmetric organization of the cell including the plasma membrane that facilitates specialized functions. Ap-BL polarity is governed by several highly conserved mechanisms including cell–cell and cell–substrate interactions that determine polarized orientation; intrinsic cues that designate specialized membrane domains (5, 6); vesicular carriers that mediate polarized secretion of protein cargo (7); sorting machinery that recognize intrinsic signals in protein cargo (8); and establishment of a unique cytoarchitecture (9, 10). Planar cell polarity (PCP), on the other hand, describes the alignment of a collection of cells within a tissue (11). In many cells including renal epithelia PCP is directly linked to sensory organelles called primary cilia (12). The basal body of the primary cilia also functions as the centrosome which duplicates and anchors mitotic spindles to control the axis of cell division necessary to form elongated epithelial tubes and branches (12, 13). The orientation of cell divisions along the axis of an epithelial tube plays a major role in nephrogenesis during kidney development (14).

The formation of renal tubules during embryogenesis requires coordinated regulation of cell polarization. Studies with epithelial cells grown on plastic or membrane filters have enlightened many key mechanisms underlying cell polarization (8, 15). However, these two-dimensional systems do not accurately recapitulate cell behaviors required to produce an epithelial tissue-like architecture. This limitation is mitigated by embedding cells in three-dimensional (3D) extracellular matrix (ECM) where they form hollow cysts lined by a single layer of polarized cells enclosing a central lumen reminiscent of cylindrical renal tubules (16). Thus 3D cell cultures have been instrumental in identifying intrinsic and extrinsic cues that regulate cell polarity during epithelial morphogenesis (13, 17). Experimental manipulations that disrupt Ap-BL polarity frequently cause defects in cyst morphology associated with defective PCP, such as formation of multiple dysfunctional lumens and misorientation of mitotic spindles, emphasizing that various aspects of cell polarity are inextricably linked (13, 16, 17). Nevertheless there are major gaps in understanding how cell

polarity is coordinated during epithelial tissue development and how its deregulation leads to different human pathologies.

The first epithelial cell sorting signals in native proteins were identified approximately 20 years ago (18-20). Since then it has emerged that membrane proteins often have multiple signals with redundant and/or opposing sorting activities (21, 22). Available evidence suggests that distinct sorting pathways enable developmental-specific patterns of membrane protein expression or transient cell polarity adjustments required to meet physiological demands (22-24). In the kidney differential expression of the epithelial specific clathrin adaptor AP1B, comprised of four protein subunits (γ, β1, μ1B, and σ), involved in BL sorting contributes to normal kidney function (25, 26). Thus AP1B is expressed in CD but not proximal tubules, allowing many BL proteins to sort to the Ap surface conceivably to optimize reabsorption of components of the ultrafiltrate (26). EGFR which is normally sorted to BL membranes in CD (27-29) has been intensely investigated as a signaling receptor with many important functions in kidney homeostasis and renal tubular repair (30). Using established monolayers of prototypical CD MDCK cells and normal mouse renal CD cells we have previously demonstrated that EGFR is trafficked to the BL membrane *via* a dileucine motif 658-LL recognized by AP1B (25, 31) (Fig. 1A). Nearly all PKD susceptibility genes abolish BL EGFR polarity (32-36) . Yet PKD mutations do not affect other AP1B-dependent cargo suggesting BL EGFR sorting has an additional level of regulation specifically disrupted in cystic cells (31).

EGFR residue Thr654 is a major protein kinase C (PKC) substrate located close to the cytoplasmic face of the plasma membrane (Fig. 1A) which negatively regulates EGFR signaling (37-40). Thr654 phosphorylation also diverts internalized EGFR from a degradative pathway to the recycling endosome in ligand stimulated CHO cells (41). We reported previously that EGFRs with a phosphomimetic T654D substitution reconstitute BL EGFR sorting in a tissue culture model for autosomal recessive PKD (31). We show here that Thr654 regulates receptor trafficking by a BL pathway independent of AP1B during formation of cell-cell junctional complexes in MDCK cells. Unexpectedly, our data have also uncovered unique roles for Thr654- and AP1B-dependent BL EGFR sorting pathways during cyst development in 3D organotypic cultures. Involvement of polarized EGFR sorting during early stages of epithelial cell polarization may provide plasticity during kidney development and repair that is also responsible for pathological manifestations in PKD. Understanding how EGFR modulates cell polarity could therefore provide very useful information to help design new therapeutic approaches to the treatment of renal diseases.

Results

EGFR residue Thr654 regulates a latent BL sorting pathway in established MDCK cell monolayers

We have shown previously that cystic cells originating from CD in the BPK model for the autosomal recessive form of PKD express AP1B and correctly sort other AP1B dependent BL cargo (31). In contrast to wild-type (WT-EGFR), EGFRs with a phosphomimetic T654D substitution [EGFR (T654D)] are targeted to BL membranes in cystic cells, suggesting T654D activates a BL sorting mechanism that supersedes the underlying EGFR trafficking

defect. This pathway has now been further characterized as follows. We first determined whether Thr654 regulates BL EGFR localization in established MDCK cell monolayers expressing equivalent levels of WT-EGFR, EGFR (T654D), or EGFR with a non-phosphorylatable T654A substitution (Supplemental Fig. 1). Steady-state membrane distributions were determined in filter-grown cells subjected to domain-specific biotinylation. Biotin immunoblotting of human EGFR immune complexes revealed that EGFRs with Thr654 substitutions were localized predominantly on BL membrane similar to WT-EGFR (Fig. 1B). In contrast, EGFR (658-AA) defective for AP1B binding (31), was associated with non-polar steady-state EGFR expression (Fig. 1B). We also demonstrated that human EGFRs were functional in all four cell lines, based on EGF-induced tyrosine phosphorylation in EGFR immune complexes (Fig. 1C). Furthermore, EGFR activity was strongly associated with BL stimulation in cells with WT-EGFR and receptors with Thr654 substitutions, in contrast to cells with nonpolarizing EGFR (658-AA) where Ap EGF also elicited robust EGFR activation.

Despite the similarities in BL EGFR membrane polarity, we did observe differences in metabolic stability amongst WT-EGFR and receptors with Thr654 substitutions. When cells were labeled with ^{35}S-amino acids and then switched to chase media for 2 to 5 h, WT-EGFR and EGFR (T654D) were metabolically stable (Fig. 1D), consistent with previous findings that EGFR has a half-life of approximately 15 h under basal conditions (28). However, EGFR (T654A) underwent limited proteolysis during the longer chase periods (Fig. 1D). The size of the major proteolytic product (labeled 150-kDa in Fig. 1D) is consistent with cleavage by endogeneous calcium-activated cytosolic calpain at one of several sites clustered in the C-terminal autophosphorylation domain of the EGFR (42). These data suggest Thr654 phosphorylation regulates a relatively minor trafficking pathway in established epithelial cells for instance during cytokinesis (43). When this signal is non-functional, EGFRs appear to be targeted for destruction by cytosolic proteases.

Cells were also examined for steady-state distribution of cell polarity markers using confocal microscopy. Images of fixed cells stained with human-specific EGFR antibody added to Ap (Fig. 2A) or BL (Fig. 2B) membranes of established epithelial cell monolayers confirmed results from the biotinylation assay in Fig. 1B. All four of the MDCK cell lines were also examined for distribution of canonical epithelial cell markers. Cells were incubated with wheat germ agglutinin (WGA), which specifically binds to N-acetylneuraminic (sialic) acids and N-acetyl-glucosamine residues in the glycocalyx located on the Ap side of MDCK cells (44), for 30 min at 37°C. WGA staining was restricted to Ap membranes in cells with WT-EGFR or EGFR (658-AA) (Fig. 2C). In contrast, cells expressing EGFRs with Thr654 substitutions also displayed WGA staining on lateral membranes most likely due to Apto-BL transcytosis during WGA labeling. However all four cell lines exhibited normal distributions of ZO-1 tight junction protein (Fig. 2D), and homotypic cell-cell adhesion molecule E-cadherin normally found on lateral membranes (Fig. 2E).

Results obtained in the MDCK cell line were verified in normal mouse CD cells using confocal microscopy (Fig. 2F). Whereas EGFR (658-AA) with a defective AP1B binding site exhibited non-polar membrane expression, WT-EGFR and EGFR (T654D) were both

located predominantly on the BL surface at steady-state. In contrast to CD cells, proximal tubule LLCPK1 cells derived from pig kidney lack functional AP1B (26, 45). Although the pig EGFR has a conserved dileucine-based signal corresponding to 658-LL in human EGFR (Fig. 1A), ectopically expressed human receptors were present on both membrane surfaces at steady state based on domain-specific EGFR staining (Fig. 2F). However, EGFR (T654D) exhibited polarized BL EGFR expression, suggesting Thr654 regulates EGFR sorting by an AP1B-independent pathway (Fig. 2F). Altogether these results confirm that AP1B regulates EGFR sorting in established CD epithelial cell monolayers. Thr654 phosphorylation appears to regulate a latent signal that is unmasked when the predominant AP1B pathway is impaired by mutations in PKD susceptibility genes or lack of AP1B expression (45, 46).

Thr654 phosphorylation regulates the predominant EGFR BL sorting pathway during formation of cell-cell junctional complexes

In order to examine the role of Thr654 on EGFR sorting during the initial acquisition of cell polarity, the next series of studies were carried out using a calcium switch model that allows control of epithelial polarization by manipulating the concentration of calcium in the extracellular media (47). Briefly, contact-naïve MDCK cells stably expressing various human EGFRs were allowed to attach to permeable filter supports in calcium-free minimal essential medium (MEM) and then switched to regular MEM with 1.8 mM calcium to initiate formation of cell-cell junctional complexes. In contrast to conventional calcium switch models where polarized membrane markers are studied 2 to 3 days after the calcium switch, we focused on the first few hours in order capture initial EGFR sorting activity. As shown in Fig. 3A, cells lacked TJ and AJ after 3 h in calcium-free medium, based on staining with antibodies to ZO-1 and E-cadherin, respectively. Furthermore, these complexes began to assemble within 90 min after MDCK cells were refed with regular MEM. We first asked if EGFRs underwent Thr654 phosphorylation in this calcium-switch model. Human EGFR immune complexes were collected at different time points after calcium addition and examined by immunoblot with phospho-specific EGFR antibodies. These antibodies were first vetted in established epithelial cell monolayers incubated with EGF or the potent PKC activator phorbol 12-myristate 13-acetate (PMA), both of which result in EGFR phosphorylation. Consistent with published literature, incubation with EGF induced phosphorylation of Thr669, which is a prominent Ser/Thr kinase substrate in ligand-stimulated cells (48), and also resulted in Tyr1173 autophosphorylation (Supplemental Fig. 2). Although Thr654 is not a kinase substrate in EGF-stimulated cells (37), Thr654 and Thr669 were both phosphorylated in the PMA-treated cells (Supplemental Fig. 2). Thr654, but not Thr669 or Tyr1173, was phosphorylated in cells cultured in calcium-free MEM by a mechanism that was reversible approximately 30 min after cells were refed with regular MEM (Fig. 3B). Furthermore, Thr654 phosphorylation was completely blocked in cells treated with the broad spectrum PKC inhibitor Gö 6983 (Fig. 3C).

We next asked whether Thr654 phosphorylation is required for EGFR BL localization in this calcium switch model using confocal microscopy. In contrast to experiments with established epithelial cell monolayers, it was not possible to carry out domain-specific EGFR staining experiments because these cultures lack junctional integrity. Thus filters were immersed in human-specific EGFR antibody to detect all membrane-exposed

receptors. BL EGFR polarity developed 1 h after cells with WT-EGFR were switched to 1.8 mM Ca^{++} (Fig. 3D). Thr654 phosphorylation peaks approximately 5 min after cells are refed with complete media well before BL WTEGFR polarity is established 3 h later. However, TJ and AJ complexes are not well-formed until the 3 h timepoint. We therefore speculate EGFRs targeted to or retained on BL membrane due to Thr654 phosphorylation diffuse to the Ap membrane until cell-cell junctions are formed. In contrast, EGFR (T654A) was predominantly localized to Ap membranes after cell-cell junction assembly at the 3 h timepoint. Apically-localized EGFR (T654A) also displayed a punctate expression pattern characteristic of Ap microvillar staining in MDCK cells at the 3 h timepoint (Fig. 3F). Consistent with a role for Thr654 phosphorylation, EGFR (T654D) was localized basolaterally similar to WT-EGFR 3 h after cells were refed with complete media (Fig. 3E). Interestingly AP1B resistant EGFR (658-AA) localized to BL membranes similar to WT-EGFR suggesting AP1B does not control EGFR sorting during assembly of new cell-cell junctional complexes (Fig. 3G). Furthermore, PKC inhibition with Gö 6983 prevented BL polarization of EGFR (658-AA) (Fig. 3G) as well as WT EGFR in contrast to EGFR (T654D) where Gö 6983 had no effect (Fig. 3H). Taken together, these data reveal that pThr654 has a dominant role in EGFR sorting during assembly of cell-cell junctional complexes.

Thr654 phosphorylation regulates BL EGFR sorting in an ATP depletion-repletion model of renal cell injury

Renal epithelial cell injury caused by ischemia and subsequent reperfusion has many adverse effects on cell polarization. Given the key role of EGFR during the recovery phase (30) we were interested in whether pThr654 regulates EGFR sorting when cell junctional integrity is re-established following renal injury. Many aspects of renal injury can be reproduced in cell culture using a combination of glycolytic and oxidative inhibitors that deplete intracellular ATP within 30 to 60 min (49, 50). Re-feeding cells with regular MEM to regenerate intracellular ATP recapitulates the regenerative phase. We therefore examined the role of Thr654 in EGFR polarization using this accepted ATP depletion-repletion model. Fig. 4A shows that ATP repletion induced cell junction reassembly within 20 min in MDCK cells expressing WT-EGFR or receptors with Thr654 substitutions based on ZO-1 and E-cadherin confocal imaging. Furthermore, Thr654 phosphorylation was rapidly and transiently induced, peaking 10 to 20 min after cells were re-fed with complete media (Fig. 4B). In contrast, intracellular ATP pools were required to return to steady-state levels of Thr669 phosphorylation seen in cells following a mock 30-min incubation in Dulbecco's-modified PBS, which initially declined and then returned to basal levels during ATP replenishment (Fig. 4B). ATP depletion-repletion had no effect on EGFR Tyr1173 autophosphorylation levels (Fig. 4B).

We next determined the fate of membrane-exposed EGFRs during ATP deletion using a biotinylation assay illustrated in Fig. 4C. Briefly, filter-grown MDCK cells were labeled from the BL surface with a membrane-impermeable, cleavable biotinylation reagent under normal growth conditions. Cells were then ATP-depleted for 30 min. Cells were either lysed immediately to determine the stability of the biotinylated proteins (T_{-ATP}), or biotin was stripped from the BL surface with 50 mM reduced glutathione ($T_{Ap + In}$). EGFR immune

complexes were then resolved by non-reducing SDS-PAGE and biotinylated EGFRs were detected by immunoblotting with a biotin antibody followed by a pan-EGFR antibody to check for protein loading. Similar to WT-EGFR, biotinylated EGFR (T654A) was present in the stripped samples, consistent with intracellular sequestration and/or BL-to-Ap transcytosis during ATP depletion (Fig. 4D - E). In contrast biotinylated EGFR (T654D) was undetectable in the stripped samples suggesting the T654D substitution promotes rapid BL EGFR recycling (Fig. 4F). Alternatively T654D may tether receptors to BL PM in cells lacking mature cell-cell junctional complexes.

The role of Thr654 on EGFR polarization in this renal injury tissue culture model was further examined by confocal microscopy. EGFR was confined to discrete Ap membrane sub-domains in all three cell lines at the end of the ATP depletion period (Fig. 5A). However, unlike cells with WT-EGFR, EGFR (T654D) displayed significant BL expression in ATP-depleted cells (Fig. 5B), consistent with results from the biotinylation assay shown in Fig. 4F. WT-EGFR and EGFR (T654D) were both localized to BL membranes 20 min after cells were refed with complete media (Fig. 5C). In contrast, EGFR (T654A) exhibited non-polar membrane expression at the 20 and 40 min time points even though cell-cell junctions had reassembled, and was not confined to BL membranes until 60 min after ATP repletion (Fig. 5A,C). We speculate that EGFR (T654A) relocalizes to the BL membrane at the 60-min time point because the AP1B-dependent pathway is now active in recycling endosomes. Thus, pThr654 also has a major role in regenerating BL EGFR expression in an established ATP depletion-repletion model of renal cell injury.

Given that the T654D substitution restores BL sorting in cystic epithelial cells (31), we also asked whether PMA treatment to activate PKC would have a similar effect. PMA promoted BL localization in cystic cells expressing WT-EGFR and EGFR with a defective 658-AA AP1B binding site (Fig. 5D). As expected, EGFR (T654D) localized to BL membranes independent of PMA treatment (Fig. 5D). These results suggest pThr654 engages BL sorting machinery that remains active even when it is not the predominant pathway for EGFR sorting during formation/reformation of cell-cell junctional complexes. Furthermore, PKC activation is sufficient to overcome deficiencies in the AP1B EGFR sorting pathway in cystic cells at least in the shortterm.

EGFR Thr654 regulates cell adhesion in 3D organotypic cultures

MDCK cells expressing Thr654 substitutions were grown in 3D organotypic cultures to investigate whether EGFR Thr654 influences epithelial cell behavior during cyst formation. Cells were stained with phalloidan and DAPI to visualize the sub-apical actin cytoskeleton and nuclei, respectively, in addition to human-specific EGFR antibody, 2 to 9 days after they were seeded in collagen gels. Cells expressing WT-EGFR gave rise to well-formed cysts with a single lumen delineated by strong sub-apical actin staining beginning at the 2 to 4 cell stage (Fig. 6A-B) on through to the late stages of cyst development (Fig. 6C). WT-EGFRs were also present exclusively on BL membranes facing the collagen gel throughout cyst development. Parental MDCK cells generated single lumen cysts of approximately the same size as cells expressing WT-EGFR (Fig. 6D). Thus EGFR overexpression *per se* does not appear to have a significant effect on cell proliferation and cyst expansion. Similar to WT-

EGFR, cells expressing EGFR (T654D) generated cysts with normal morphology, single lumen formation, and BL EGFR expression at early and late stages of cyst growth (Fig. 7A-C). In sharp contrast, EGFR (T654A) expression severely affected cyst formation. This mutant receptor co-localized with actin at nascent Ap membrane at the 2-cell state (Fig. 7D). Cells then began to acquire a mesenchymal-like shape with uniform EGFR membrane staining and filopodial-like extensions after 1 or 2 cell divisions (Fig. 7E). The presumptive cysts that were formed at later stages were dysmorphic containing cells of diverse shape and size instead of cuboidal epithelial cells observed in cysts formed by WT-EGFR or EGFR (T654D)-expressing cells (Fig. 7F). These presumptive cysts appeared to have rudimentary luminal structures although they lacked significant sub-apical actin cytoskeleton (see asterisks in Fig. 7F). Different MDCK sub-clones can exhibit variable phenotypes in collagen gels (33). However, the aberrant phenotype in Fig. 7F was noted in two independent MDCK cell lines expressing EGFR (T654A), ruling out the possibility that the EGFR (T654A) phenotype was due to clonal selection.

BL EGFR delivery via the AP1B-dependent pathway has an essential role in lumen formation in 3D organotypic culture

We next sought to determine the effect of defective AP1B EGFR sorting in MDCK cells grown in collagen gels. Similar to WT-EGFR, EGFR (658-LL) localized to BL membrane facing the ECM at the 2-cell stage (Fig. 8A). In contrast to cells with EGFR (T654A), EGFR (658-AA) expression was not associated with any overt effects on cell adhesion following subsequent cells divisions (Fig. 8B-E). However, cysts began to display multiple nascent Ap membrane initiation sites as indicated by actin staining after the two-cell stage (Fig. 8B-D), and cysts had multiple misshapen lumens after 9 days in culture (Fig. 9E). Furthermore, EGFR (658-AA) receptors were predominantly co-localized with sub-apical actin cytoskeleton after the 2-cell stage consistent with missorting in the AP1B-dependent pathway. Altogether our data suggest that cells utilize the pThr654 BL EGFR sorting pathway initially and then switch to the AP1B-dependent pathway after cell-cell junctions have assembled in collagen gels. Furthermore, each pathway has a critical role at different stages of cyst development.

AP1B sorts EGFRs predominantly in the biosynthetic route in MDCK cells

Recycling endosomes constitute a critical post-Golgi sorting route for some BL membrane proteins (22, 51). Thus AP1B can sort cargo in both biosynthetic and recycling routes by virtue of its functional localization to recycling endosomes (52). The following experiments determined the AP1B sorting route for EGFR in established epithelial cell monolayers. We first established sorting routes for newly synthesized EGFRs. Briefly, cells grown at confluence for 5 days were pulse-labeled with ^{35}S-amino acids for 15 min, switched to chase medium with an excess of non-radioactive amino acids up to 90 min, biotinylated at Ap or BL surfaces, and EGFRs were recovered by sequential immunoprecipitation and streptavidin purification. Similar to newly synthesized WT-EGFR, EGFRs with T654A or T654D substitutions were delivered directly to the BL membrane (Fig. 9A-C). In contrast, newly synthesized AP1B-defective EGFR (658-AA) exhibited nonpolar membrane delivery (Fig. 9D). We next determined the extent to which EGFRs lacking an AP1B binding site undergo transcytosis to Ap membrane following BL delivery. This was accomplished using

domain-specific biotin cleavage to determine the fate of basolaterally biotinylated EGFR according to the protocol in Fig. 9E. Briefly, filter-grown MDCK cells were labeled from the BL surface with the cleavable biotinylation reagent and then incubated for 4 h at 37°C. Cells were either lysed immediately to determine the stability of the biotinylated proteins (T_{4h}), or biotin was stripped off from the Ap surface only ($T_{BL + In}$), from both the Ap and BL surfaces (T_{In}), or from the BL surface only ($T_{Ap + In}$). Human EGFR immune complexes were then analyzed by immunoblotting with a biotin-specific antibody to detect receptors that were labeled with biotin at the beginning of the experiment, or with a pan-EGFR antibody to check for protein loading. As expected, biotin was removed from WT-EGFR only when the stripping solution was added to the BL surface consistent with BL EGFR targeting (Fig. 9F). Similar results were obtained in cells expressing EGFR (658-AA), suggesting AP1B-defective receptors do not undergo significant BL-to-Ap transcytosis (Fig. 9G). Altogether our results are consistent with a model where AP1B sorts BL EGFR in the biosynthetic route of established MDCK cell monolayers. We cannot exclude the possibility that AP1B also regulates low levels of constitutive BL recycling under basal conditions similar to other AP1B dependent cargo (52).

Discussion

Our studies have identified two functionally distinct BL EGFR sorting pathways, one regulated by Thr654 that primarily functions during formation of new TJ and AJ complexes and a second AP1B-dependent route that is the predominant pathway after cell-cell junctions are assembled. The model that best fits our data is shown in Fig. 10. Based on our previous finding that EGFR (T654D) co-localizes with intracellular $Rab11^+$ vesicles (31) and data presented in this manuscript, we hypothesize that EGFRs are sequestered in $Rab11^+$ endosomes in epithelial cells lacking functional cell-cell junctional complexes. EGFRs then recycle to BL membrane by a mechanism involving PKC-dependent Thr654 phosphorylation once these junctional complexes begin to assemble (Fig. 10A). Although Thr654 phosphorylation is required, we cannot exclude the possibility that additional factors contribute to EGFR sorting in polarizing cells. While pThr654 could interact directly with BL sorting machinery, it is conceivable it alters EGFR conformation to unmask a sorting signal located some distance away for instance the previously identified 667-PLTP BL sorting signal (27). The sequestered receptors are presumably sorted away from membrane proteins *en route* from the endoplasmic reticulum (ER) to Ap plasma membrane *via* passage through common recycling endosome intermediate (53). This circuit may also represent an alternative N-glycan dependent EGFR Ap sorting route in cells lacking an active BL sorting program (29). Several outstanding questions remain: *i*) Does Thr654 phosphorylation activate a latent BL signal and if so what are its molecular characteristics? *ii*) Is the PKC isoform responsible for modifying Thr654 specifically activated in $Rab11^+$ recycling endosomes in cells lacking cell-cell junctional complexes? *iii*) How is PKC activated? *iv*) How does the Thr654-dependent sorting route differ from the canonical AP1B-dependent BL pathway?

We have also demonstrated that the previously identified AP1B dependent pathway (31) sorts EGFRs in a biosynthetic route most likely *via* post-TGN endosome sorting intermediates (Fig. 10B). This is consistent with a previous report that a membrane-

permeate competing peptide encompassing 658-LL blocks EGFR sorting from the TGN to the BL membrane domain in MDCK cells (54). In this regard EGFR is similar to VSV G-protein (VSVG) which is also transported to BL membranes along an AP1B-biosynthetic route (52, 55, 56). For other membrane cargo, notably transferrin and LDL receptors, AP1B exerts its sorting role in the recycling route and not the biosynthetic route (52) (56). AP1B-dependent VSVG sorting is mediated by a consensus YXXΦ BL sorting motif recognized by the AP1B μ1B-subunit (57). In contrast the AP1B signal in EGFR is a dileucine motif which may be recognized by γ and δ1 subunits acting together (58, 59). However, the EGFR 658-LL signal does not conform to consensus dileucine motifs which have an N-terminal acidic residue [i.e., D/ExxxL(L/I)]. Thr654 could regulate AP1B-dependent sorting by providing an acidic charge in its phosphorylated state. However, pThr654 must also regulate an AP1B-independent pathway since EGFR (T654D) sorts basolaterally in AP1B-deficient LLCPK1 cells. Our original studies identifying 658-LL as an AP1B binding site were carried out by adding purified clathrin adaptors to GST fusion proteins with WT and mutant EGFR juxtamembrane sequences (31). Identification of AP subunits required for this interaction is an important area for future investigation particularly if 658-LL represents a new class of unconventional AP1B recognition motifs.

The report that EGFR missorts in AP1B-deficient LLCPK1 cells is seemingly at odds with previous reports that BL but not Ap EGF induces DNA synthesis in this cell line (60). These studies were carried in cells expressing physiological levels of endogenous pig EGFR following a brief 30 sec exposure to EGF. However, it has also been reported that overexpressed human EGFRs are activated on both membrane surfaces of LLCPK1 cells (61). Although it is possible that the pig receptor has a novel BL sorting signal not found in human EGFR, Thr654 and 658-LL are both highly conserved in mammalian cells (Fig. 1A). The fact that EGFR (T654D) sorts basolaterally in LLCPK1 cells argues that the alternative Thr654-dependent sorting machinery is active, raising two possibilities. First, this is the predominant route utilized by endogenous pig EGFR but PKC-mediated Thr654 phosphorylation is rate-limiting leading to EGFR missorting in an AP1B-dependent pathway when the receptor is overexpressed. Second, there is also precedence that membrane cargo can switch between different sorting routes as a function of confluency and time in culture. For instance, the study in (60) employed LLCPK1 cells seeded on filters that were pre-coated with collagen which could have affected their differentiation status. It will be interesting to ascertain if different BL sorting pathways are utilized along the length of the nephron to regulate segment-specific EGFR function. Thus the Thr654-dependent pathway may be the predominant pathway in proximal tubules, in contrast to AP1B which is the main driver of BL sorting in CD. If true, this suggests EGFR sorting in proximal tubules is highly sensitive to PKC signaling pathways.

Several lines of evidence suggest the AP1B EGFR sorting pathway does not have a significant role before cell-cell junctions are formed. The AP1B pathway cannot over-ride the T654A mutation that impairs EGFR polarity in calcium-switch and ATP depletion-repletion models. Furthermore AP1B-defective EGFR (658-AA) initially distributes to BL membranes in both these models by a mechanism requiring PKC. These findings suggest that EGFR traffics through an AP1B-inaccessible compartment, that AP1B is functionally inhibited, or that the EGFR 658-LL signal is masked in epithelial cells lacking intact cell-

cell junctions. Interestingly, a T654D substitution disrupts *in vitro* binding of the EGFR juxtamembrane peptide depicted in Fig. 1A to intact AP1B complexes in GST pull-down assays (31). It is therefore conceivable that pThr654 mediates a switch between redundant BL sorting pathways by simultaneously suppressing AP1B dependent EGFR sorting and activating a latent signal employed during epithelial morphogenesis. Although additional testing is needed, structural studies indicate that Thr654 and 658-LL reside in highly flexible segments of the juxtamembrane region which could potentially interact to modulate EGFR sorting in the context of the native protein (62).

Cells comprising the metanephric mesenchyme undergo mesenchymal-to-epithelial transition giving rise to an epithelial structure called the renal vesicle during kidney development (63). A hallmark of epithelial morphogenesis is the *de novo* formation of a central lumen that in this case ultimately forms the interconnected luminal network of the nephron and CD system. Several tissue culture models including growth of MDCK cells in collagen gels have been employed to identify mechanisms underlying cell polarity and *de novo* epithelial lumen formation (16). Surprisingly, different BL EGFR sorting routes are associated with very distinct phenotypes in cyst-forming assays. EGFR (T654A) expression promotes EGFR missorting and severely compromises epithelial cell-cell or cell-matrix adhesion during the early stages of cyst development. In contrast EGFR (658-AA) sort to the BL membrane initially, but then exhibits polarity defects associated with aberrant lumen formation upon subsequent cell divisions when cell-cell junctions do not fully dissociate (64). These phenotypes have several possible explanations that are not mutually exclusive. The Thr654-dependent sorting route may target EGFRs to membrane domains that designate new sites of cell adhesion complex assembly (5, 6, 65). Alternatively, the Thr654-dependent EGFR sorting route could maintain the functional integrity of $Rab11^{+}$ recycling endosomes which are necessary for E-cadherin trafficking to AJ (66). In keeping with this hypothesis, the finding that Ap glycocalyx mislocalizes to BL membrane in cells with EGFR (T654D) or EGFR (T654A) suggests Thr654-dependent EGFR sorting must be kept within a certain threshold for correct function of Ap recycling endosomes. In contrast, the AP1B-dependent sorting route may exclude EGFR from the Ap domain where it suppresses recruitment of protein complexes involved in lumen formation. Alternatively the AP1B-dependent sorting route could target EGFR to BL subdomains involved in cell signaling that then control *de novo* lumen formation.

Do our data provide any insights to the role of EGFR in epithelial cell development? EGFR −/− knockout mice display strain-dependent defects in epithelial development in several organs including kidney, skin, lung, and the gastrointestinal tract (67, 68). More recently targeted EGFR inactivation has revealed critical roles for EGFR in discrete nephron segments and CD. EGFR inactivation in proximal tubules delays recovery from acute renal injury (69). If Thr654-dependent sorting is the predominant sorting pathway in proximal tubules with physiological levels of the endogenous receptor, then EGFR could have a major role restoring cell-cell junctions during the recovery phase. EGFR is also highly expressed in ureteric bud (UB) which gives rise to the CD system (63). Targeted inactivation in UB suggests EGFR functions primarily to drive elongation of emerging CD and optimize urine-concentrating ability (70). This finding is consistent with our results that EGFR sorting *via*

an AP1B dependent pathway integrates Ap-BL polarity with PCP in collagen gels. It is also thought that lumen formation during tubulogenesis involves transient formation of lateral lumina that progressively relocate to the Ap domain (71). Our data suggest EGFR could participate in this transient stage of epithelial morphogenesis by two mechanisms: First by regulating lateral membrane architecture *via* the Thr654-dependent sorting pathway; and second by generating intrinsic cues for relocating the lateral lumina to the Ap surface following a developmental switch to the AP1B-dependent pathway.

The EGFR missorting phenotype associated with PKD is generally assumed to drive cell proliferation required for cyst expansion because of enhanced EGFR signaling activity (46). The data in this manuscript suggest that abnormal EGFR sorting may also contribute to dysfunction of molecular networks that control cell adhesion and integrate Ap-BL polarity and PCP required for lumen formation. Thus EGFR missorting could also have a critical role in pre-cystic kidneys. In addition, our data indicate that cystic cells do not engage the AP1B-dependent BL EGFR sorting program employed in epithelial cells with established apico-basolateral polarity. Because cystic cells do not exhibit global AP1B sorting abnormalities, EGFR passage through this route may have an additional level of regulation not required for other AP1B cargoes. In future studies, it is likely that the novel PKD cell models will aid in the discovery of fundamental new cell biological mechanisms involved in EGFR sorting.

Materials and Methods

Antibodies and reagents

The following antibodies were purchased: E-cadherin mouse monoclonal antibody, BD Biosciences (San Diego, CA) and Abcam (Cambridge, MA), respectively; EGFR rabbit polyclonal antibody, Research Diagnostic (Flanders, N.J); mouse-specific EGFR goat polyclonal antibody, R & D Systems (Minneapolis, MN); phospho-specific EGFR (Thr669) mouse monoclonal antibody, Millipore (Billerica, MA); HRP-conjugated anti-phosphotyrosine antibody, BD Transduction Laboratories (Lexington, KY); and HRP-conjugated biotin mouse monoclonal antibody and phospho-specific EGFR (Tyr1173) rabbit polyclonal antibody, Cell Signaling (Beverly MA). ZO-1 rat monoclonal antibody was obtained from Developmental Studies Hybridoma Bank developed under the auspices of NICHD and maintained by The University of Iowa Department of Biological Sciences (Iowa City, IA). Human-specific EGFR1 mouse monoclonal antibody (72) was produced using a standard ascites method. Conjugated secondary antibodies were purchased from Jackson ImmunoResearch Laboratories (Fort Washington, PA), biotin and streptavidin reagents from Pierce (Rockland, IL), receptor-grade mouse EGF and PMA from Sigma, Gö 6983 from EMD Chemicals (Gibbstown, NJ), blue-fluorescent DAPI nucleic acid counterstain and Alexa Fluor 488 WGA from Molecular Probes (Eugene, OR), and phalloidin (rhodamine) from Cytoskeleton, Inc. (Denver, CO).

Cells and cell culture

Canine MDCK renal epithelial cells expressing human WT-EGFR or human EGFRs with T654D or 658-LL dialanine substitutions were described previously (28, 29). MDCK cells were co-transfected with a cDNA encoding human EGFR with a T654A substitution cloned

in the eukaryotic expression plasmid pRT3 described in (73) in a 10:1 ratio with pSV2-neo (American Type Tissue Culture Collection). Stable cell lines were selected with G418 (0.8 mg/ml Geneticin; Gibco-BRL) for 10 days followed by 3 sequential rounds of sterile sorting on a flow cytometer (Cytofluorograph IIs; Ortho Instruments, Westwood, MA) after cells were stained with the human-specific EGFR1 antibody (29). All MDCK-related cell lines were maintained in MEM supplemented with 10% FBS. Pig-derived proximal tubule LLCPK1 and mouse-derived CD cell lines from the BPK ARPKD model and age-matched normal littermates expressing human EGFR constructs were described previously (31).

Generating stable epithelial cell monolayers

For studies in established monolayers, confluent cells were split and seeded on polycarbonate Transwell filter inserts (0.4 μm pore size; Costar Corp, Cambridge, MA) at high density (3.0×10^5 cells/cm^2). Filters were refed 24 h later to remove cell debris, and then every other day. Electrically resistant monolayers suitable for domain-specific assays were ready for use 4 to 5 days later for MDCK- and mouse CD-derived cells, and 8 to 9 days later for LLCPK-derived cells.

Calcium switch model

Cells were trypsinized and seeded at low density on two consecutive days. The contact-naïve cells were then seeded at high density (3.0×10^5 cells/cm^2) on permeable filter supports in MEM without $CaCl_2$ (Spinner Modification; Sigma) supplemented with 10% dialyzed FBS. Cells were re-fed with regular growth medium containing 1.8 mM Ca^{++} three h later to initiate formation of junctional complexes.

ATP depletion-repletion model

Mature monolayers were incubated in PBS supplemented with 1.5 mM $CaCl_2$, 2 mM $MgCl_2$, and a combination of glycolytic (2 mM 2-deoxy-d-glucose) and oxidative (10 mM antimycin A) ATP inhibitors for 30 min to deplete ATP. ATP levels were restored by re-feeding cells with regular MEM supplemented with 10% FBS.

3D organotypic culture

3D cultures were prepared according to published methods (5, 74). Briefly, cells were diluted in type I collagen (*PureCol*®, bovine collagen at 3 mg/ml; Advanced Biomatrix; San Diego, CA) at a density of 4×10^4 cells/ml. Cell-collagen solutions were allowed to gel at 37°C before medium was added. Media was replenished every 3 d until cyst morphology was examined by confocal microscopy. Collagen gels were treated with collagenase type VII (Sigma C-2399) at 100 U/ml in PBS supplemented with 1 mM $CaCl_2$ for 15 min at 37°C to increase the accessibility of antibodies to cysts.

Immunoprecipitation, immunoblotting

Cells were lysed with a solution of 1% (w/v) Triton X-100 in 20 mM Tris, pH 8.0, 50 mM NaCl, 5 mM EDTA, 0.2% BSA, 0.2 mM phenylmethylsulfonyl fluoride, and 1 mM leupeptin (IP buffer). Immunoprecipitations were carried out using antibodies adsorbed to protein A-Sepharose CL-4B beads (Sigma). Immune complexes containing biotinylated

proteins were boiled for 5 min in 100 μl of 10% SDS and SDS-protein solutions were brought to 1 ml with IP buffer and incubated with streptavidin-agarose beads for 16 h at 4°C. Affinity-purified protein complexes were eluted with Laemmli sample buffer and resolved by SDS-PAGE. Gels with radioactive proteins were treated with En^3Hance (PerkinElmer-NEN, Wilmington, DE) for fluorography. Non-radioactive affinity-purified protein complexes or equal aliquots of total cellular protein were resolved by SDS-PAGE and transferred to nitrocellulose membranes using standard methods. Nitrocellulose membranes were incubated with primary antibodies followed by HRP-conjugated secondary antibodies for detection by enhanced chemiluminescence (Amersham-Pharmacia).

Pulse-chase-biotinylation experiments

Filter-grown cells were pre-incubated in methionine and cysteine-free MEM for 1 h. The amino acid-starved cells were pulse-labeled from the BL surface with ^{35}S-Express Protein Labeling Mix (2.5 mCi/ml; PerkinElmer Life Sciences, Boston, MA) diluted in amino acid-deficient MEM supplemented with 10% dialyzed FBS and 0.2% BSA. The radio-labeled cells were then incubated at 37°C in MEM supplemented with a 10-fold excess of non-radioactive methionine and cysteine (chase medium). For biotinylation, cells were rinsed three times with PBS supplemented with 1 mM $CaCl_2$ and 1 mM $MgCl_2$ (PBS-CM) and then incubated for 30 min at 4°C with EZ-Link (1 mg/ml; Pierce Chemical Company; Rockford, IL) dissolved in PBS-CM added to Ap or BL surface. The reaction was quenched with 50 mM NH_4Cl and cells were lysed with IP buffer.

Intracellular sequestration, transcytosis assays

Filter-grown cells were incubated with EZ-Link sulfo-NHS-SS-biotin™ (1 mg/ml; Pierce) dissolved in PBSCM added to the BL side for 30 min on ice. Cells were rinsed three times with 100 mM glycine in PBSCM to quench excess biotin and then harvested immediately or following ATP depletion or a 4-h incubation at 37°C, or to assess intracellular sequestration or BL-to-Ap transcytosis, respectively. Figs. 4C and 8E show detailed protocols for both these assays. Cell surface biotin was stripped off by incubating cells twice with 155 mg of reduced glutathione (Sigma) in 9 ml of 83 mM NaCl supplemented with 1 ml FBS, 1 mM each of $CaCl_2$ and 1 mM $MgCl_2$, and 60 μl of 50% NaOH solution for 20 min on ice. Cells were incubated twice for 15 min each with ice-cold 50 mM iodoacetimide in PBS-CM to quench excess glutathione. EGFR immune complexes were resolved by non-reducing SDS-PAGE and immunoblotted with HRP-conjugated biotin antibody.

Confocal microscopy

Samples were perforated with 0.5% β-escin in a solution of 80 mM PIPES, pH 6.8, supplemented with 5 mM EGTA and 1 mM $MgCl_2$ for 5 min and fixed with 3% paraformaldehyde–PBS for 15 min (75). Samples were blocked with a solution containing 1% normal serum from the host animal used to generate secondary antibodies. Cells were stained with primary or secondary antibodies diluted in a solution containing 0.5% β-escin and 3% RIA-grade BSA at 4°C overnight or 1 h at room temperature. Alternatively cells were fixed with 3% paraformaldehyde–PBS for 15 min and stained with antibodies that detect extracellular epitopes without permeabilization (29). Some samples were labeled with Alexa Fluor 488 WGA at 37°C for 30 min prior to processing to visualize Ap membranes.

Cells were optically sectioned with a Zeiss LSM 510 Meta laser scanning microscope equipped with argon and helium-neon lasers (Carl Zeiss MicroImaging, Jenna, Germany). Image resolution with Zeiss 63 × or 100 × oil immersion objectives and Zeiss LSM software was 1024 × 1024 pixels.

Image preparation

Digital images were prepared using Adobe Photoshop® CS4 and Adobe Illustrator® CS5.1 software packages.

Supplementary Material

Refer to Web version on PubMed Central for supplementary material.

Acknowledgements

C.R.C. was supported by NIH grant RO1 GM081498 and C.U.C. by P30 DK27651. This work was also supported by NIH grant P50 DK54178 (C.R.C. and C.U.C.). M.E.H. and S.R. were supported by NIH T32 grants HL07717 and HL007415, respectively. We wish to thank members of the Carlin and Cotton laboratories for many useful discussions.

Abbreviations

AJ	*adherens* junction
Ap	apical
BL	basolateral
CD	collecting duct
3D	three-dimensional
ECM	extracellular matrix
EGFR	epidermal growth factor receptor
ER	endoplasmic reticulum
MEM	minimal essential medium
PKC	protein kinase C
PKD	polycystic kidney disease
PMA	phorbol 12-myristate 13-acetate
TGN	*trans*-Golgi network
TJ	tight junction
UB	ureteric bud
VSVG	vesicular stomatitis virus glycoprotein
WGA	wheat germ agglutinin
WT	wild-type

References

1. Alpern, R.; Hebert, S., editors. Seldin and Giebisch's The Kidney. Fourth ed.. Elsevier Academic Press; Boston: 2007.
2. Brown D, Stow JL. Protein trafficking and polarity in kidney epithelium: from cell biology to physiology. Physiological Reviews. 1996; 76(1):245–297. [PubMed: 8592730]
3. National KaUDC. USRDS 2009 Annual Data Report. 2009. http://kidney.niddk.nih.gov/
4. Torres VE, Boletta A, Chapman A, Gattone V, Pei Y, Qian Q, Wallace DP, Weimbs T, Wulthrich RP. Prospects for mTOR inhibitor use in patients with polycystic kidney disease and hamartomatous diseases. Clin J Am Soc Nephrol. 2010; 5(7):1312–1329. [PubMed: 20498248]
5. Bryant DM, Datta A, Rodriguez-Fraticelli AE, Peranen J, Martin-Belmonte F, Mostov KE. A molecular network for de novo generation of the apical surface and lumen. Nat Cell Biol. 2010; 12(11):1035–1045. [PubMed: 20890297]
6. Gassama-Diagne A, Yu W, ter Beest M, Martin-Belmonte F, Kierbel A, Engel J, Mostov K. Phosphatidylinositol-3,4,5-trisphosphate regulates the formation of the basolateral plasma membrane in epithelial cells. Nat Cell Biol. 2006; 8(9):963–970. [PubMed: 16921364]
7. Rodriguez-Boulan E, Kreitzer G, Musch A. Organization of vesicular trafficking in epithelia. Nat Rev Mol Cell Biol. 2005; 6(3):233–247. [PubMed: 15738988]
8. Nelson WJ, Rodriguez-Boulan E. Unravelling protein sorting. Nat Cell Biol. 2004; 6(4):282–284. [PubMed: 15057238]
9. Yeaman C, Grindstaff KK, Nelson WJ. New perspectives on mechanisms involved in generating epithelial cell polarity. Physiol Rev. 1999; 79:73–98. [PubMed: 9922368]
10. Stein M, Wandinger-Ness A, Roitbak T. Altered trafficking and epithelial cell polarity in disease. Trends Cell Biol. 2002; 12(8):374–378. [PubMed: 12191914]
11. Gray RyanÂ S, Roszko I, Solnica-Krezel L. Planar cell polarity: Coordinating morphogenetic cell behaviors with embryonic polarity. Dev Cell. 2011; 21(1):120–133. [PubMed: 21763613]
12. Fischer E, Pontoglio M. Planar cell polarity and cilia. Sem Cell Dev Biol. 2009; 20:998–1005.
13. Rodríguez-Fraticelli AE, Galvez-Santisteban M, Martin-Belmonte F. Divide and polarize: recent advances in the molecular mechanism regulating epithelial tubulogenesis. Curr Opin Cell Biol. 2011; 23(5):638–646. [PubMed: 21807489]
14. McNeill H. Planar cell polarity and the kidney. J Am Soc Nephrol. 2009; 20(10):2104–2111. [PubMed: 19762494]
15. Rodriguez-Boulan E, Nelson WJ. Morphogenesis of the polarized epithelial cell phenotype. Science. 1989; 245:718–725. [PubMed: 2672330]
16. O'Brien LE, Zegers MMP, Mostov KE. Building epithelial architecture: insights from three-dimensional culture models. Nat Rev Mol Cell Biol. 2002; 3(7):531–537. [PubMed: 12094219]
17. Martin-Belmonte F, Mostov K. Regulation of cell polarity during epithelial morphogenesis. Current Opinion in Cell Biology. 2008; 20(2):227–234. [PubMed: 18282696]
18. Brown DA, Crise B, Rose JK. Mechanisms of membrane anchoring affects polarized expression of two proteins in MDCK cells. Science. 1989; 245:1499–1501. [PubMed: 2571189]
19. Casanova JE, Apodaca G, Mostov KE. An autonomous signal for basolateral sorting in the cytoplasmic domain of the polymeric immunoglobulin receptor. Cell. 1991; 66:65–75. [PubMed: 2070419]
20. Matter K, Hunziker W, Mellman I. Basolateral sorting of LDL receptor in MDCK cells: the cytoplasmic domain contains two tyrosine-dependent targeting determinants. Cell. 1992; 71:741–753. [PubMed: 1423629]
21. Mellman I, Nelson WJ. Coordinated protein sorting, targeting and distribution in polarized cells. Nat Rev Mol Cell Biol. 2008; 9(11):833–845. [PubMed: 18946473]
22. Heike F, Polly EM, Ora AW. Taking the Scenic Route: Biosynthetic Traffic to the Plasma Membrane in Polarized Epithelial Cells. Traffic. 2009; 10(8):972–981. [PubMed: 19453969]
23. Matter K, Mellman I. Mechanisms of cell polarity: sorting and transport in epithelial cells. Curr Opin Cell Biol. 1994; 6:545–554. [PubMed: 7986532]

24. Mostov KE, Cardone MH. Regulation of protein traffic in polarized epithelial cells. Bioessays. 1995; 17:129–138. [PubMed: 7748163]
25. Fölsch H. The building blocks for basolateral vesicles in polarized epithelial cells. Trends Cell Biol. 2005; 15:222–228. [PubMed: 15817379]
26. Schreiner R, Frindt G, Diaz F, Carvajal-Gonzalez JM, Perez Bay AE, Palmer LG, Marshansky V, Brown D, Philp NJ, Rodriguez-Boulan E. The absence of a clathrin adapter confers unique polarity essential to proximal tubule function. Kidney Int. 2010; 78(4):382–388. [PubMed: 20531453]
27. He C, Hobert M, Friend L, Carlin C. The epidermal growth factor receptor juxtamembrane domain has multiple basolateral plasma membrane localization determinants, Including a dominant signal with a polyproline core. J Biol Chem. 2002; 277(41):38284–38293. [PubMed: 12161422]
28. Hobert M, Carlin C. Cytoplasmic juxtamembrane domain of human EGF receptor is required for basolateral localization in MDCK cells. J Cell Physiol. 1995; 162:434–446. [PubMed: 7860650]
29. Hobert ME, Kil S, Carlin CR. The cytoplasmic juxtamembrane domain of the epidermal growth factor receptor contains a novel autonomous basolateral sorting signal. J Biol Chem. 1997; 272:32901–32909. [PubMed: 9407068]
30. Zeng F, Singh AB, Harris RC. The role of the EGF family of ligands and receptors in renal development, physiology and pathophysiology. Experimental Cell Research. 2009; 315(4):602–610. [PubMed: 18761338]
31. Ryan S, Verghese S, Cianciola NL, Cotton CU, Carlin CR. Autosomal recessive polycystic kidney disease epithelial cell model reveals multiple basolateral epidermal growth factor receptor sorting pathways. Mol Biol Cell. 2010; 21(15):2732–2745. [PubMed: 20519437]
32. Du J, Wilson PD. Abnormal polarization of EGF receptors and autocrine stimulation of cyst epithelial growth in human ADPKD. Am J Physiol. 1995; 269(2 Pt 1):C487–C495. [PubMed: 7653531]
33. Orellana SA, Sweeney WE, Neff CD, Avner ED. Epidermal growth factor receptor is abnormal in murine polycystic kidney. Kidney Int. 1995; 47:490–499. [PubMed: 7723235]
34. Yoder BK, Richards WG, Sommardahl C, Sweeney WE, Michaud EJ, Wilkinson JE, Avner ED, Woychik RP. Functional correction of the renal defects in a mouse model for ARPKD through expression of the cloned wild-type Tg737 gene. Kidney Int. 1996; 50:1240–1248. [PubMed: 8887283]
35. Sweeney WE, Kusner L, Carlin CR, Chang S, Futey L, Cotton CU, Dell KM, Avner ED. Phenotypic analysis of conditionally immortalized cells isolated from the BPK model of ARPKD. Am J Physiol. 2001; 281:C1695–C1705.
36. Lin F, Hiesberger T, Cordes K, Sinclair A, Goldstein L, Somlo S, Igarashi P. Kidney-specific inactivation of the KIF3A subunit of kinesin-II inhibits renal ciliogenesis and produces polycystic kidney disease. Proc Natl Acad Sci. 2003; 100:5286–5291. [PubMed: 12672950]
37. Hunter T, Ling N, Cooper JA. Protein kinase C phosphorylation of the EGF receptor at a threonine residue close to the cytoplasmic face of the plasma membrane. Nature; 1985; 311:480–483.
38. Beguinot L, Hanover JA, Ito S, Richert ND, Willingham MC, Pastan I. Phorbol esters induce transient internalization without degradation of unoccupied epidermal growth factor receptor. Proc Natl Acad Sci USA. 1985; 82:2774–2778. [PubMed: 2859591]
39. Davis RJ, Czech MP. Platelet-derived growth factor mimics phorbol diester action on epidermal growth factor receptor phosphorylation at threonine-654. Proc Natl Acad Sci. 1985; 82(12):4080–4084. [PubMed: 2987962]
40. Lund KA, Lazar CS, Chen WS, Walsh BJ, Welsh JB, Herbst JJ, Walton GM, Rosenfeld MG, Gill GN, Wiley HS. Phosphorylation of the epidermal growth factor receptor at threonine 654 inhibits ligand-induced internalization and down-regulation. J Biol Chem. 1990; 265:20517–20523. [PubMed: 2173710]
41. Bao J, Alroy I, Waterman H, Schejter ED, Brodie C, Gruenberg J, Yarden Y. Threonine phosphorylation diverts internalized epidermal growth factor receptors from a degradative pathway to the recycling endosome. J Biol Chem. 2000; 275:26178–26186. [PubMed: 10816576]
42. Gregoriou M, Willis AC, Pearson MA, Crawford C. The calpain cleavage sites in the epidermal growth factor receptor kinase domain. Eur J Biochem. 1994; 223(2):455–464. [PubMed: 8055914]

43. Schluter MA, Pfarr CS, Pieczynski J, Whiteman EL, Hurd TW, Fan S, Liu C-J, Margolis B. Trafficking of Crumbs3 during cytokinesis is crucial for lumen formation. Mol Biol Cell. 2009; 20(22):4652–4663. [PubMed: 19776356]
44. Kovbasnjuk ON, Spring KR. The apical membrane glycocalyx of MDCK cells. J Membrane Biol. 2000; 176(1):19–29. [PubMed: 10882425]
45. Fölsch H, Ohno H, Bonifacino JS, Mellman I. A novel clathrin adaptor complex mediates basolateral targeting in polarized epithelial cells. Cell. 1999; 99:189–198. [PubMed: 10535737]
46. Wilson PD. Apico-basal polarity in polycystic kidney disease epithelia. Biochim Biophys Acta - Mol Basis Dis. 2011; 1812(10):1239–1248.
47. Gumbiner B, Simons K. A functional assay for proteins involved in establishing an epithelial occluding barrier: identification of a uvomorulin-like polypeptide. The Journal of Cell Biology. 1986; 102(2):457–468. [PubMed: 3511070]
48. Countaway JL, Northwood IC, Davis RJ. Mechanism of phosphorylation of the epidermal growth factor receptor at threonine 669. J Biol Chem. 1989; 264:10828–10835. [PubMed: 2543683]
49. Mandel LJ, Bacallao R, Zampighi G. Uncoupling of the molecular 'fence' and paracellular 'gate' functions in epithelial tight junctions. Nature. 1993; 361(6412):552–555. [PubMed: 8429911]
50. Bacallao R, Garfinkel A, Monke S, Zampighi G, Mandel LJ. ATP depletion: a novel method to study junctional properties in epithelial tissues. I. Rearrangement of the actin cytoskeleton. J Cell Sci. 1994; 107(12):3301–3313. [PubMed: 7706387]
51. Gonzalez A, Rodriguez-Boulan E. Clathrin and AP1B: Key roles in basolateral trafficking through transendosomal routes. FEBS Letters. 2009; 583:3784–3795. [PubMed: 19854182]
52. Gravotta D, Deora A, Perret E, Oyanadel C, Soza A, Schreiner R, Gonzalez A, Rodriguez-Boulan E. AP1B sorts basolateral proteins in recycling and biosynthetic routes of MDCK cells. Proc Natl Acad Sci. 2007; 104(5):1564–1569. [PubMed: 17244703]
53. Weisz OA, Rodriguez-Boulan E. Apical trafficking in epithelial cells: signals, clusters and motors. J Cell Sci. 2009; 122(23):4253–4266. [PubMed: 19923269]
54. Soza A, Norambuena A, Cancino J, de la Fuente E, Henklein P, Gonzalez A. Sorting competition with membrane-permeable peptides in intact epithelial cells revealed discrimination of transmembrane proteins not only at the trans-Golgi network but also at pre-Golgi stages. J Biol Chem. 2004; 279(17):17376–17383. [PubMed: 14764609]
55. Ang AL, Taguchi T, Francis S, Folsch H, Murrells LJ, Pypaert M, Warren G, Mellman I. Recycling endosomes can serve as intermediates during transport from the Golgi to the plasma membrane of MDCK cells. J Cell Biol. 2004; 167(3):531–543. [PubMed: 15534004]
56. Cancino J, Torrealba C, Soza A, Yuseff MI, Gravotta D, Henklein P, Rodriguez-Boulan E, Gonzalez A. Antibody to AP1B adaptor blocks biosynthetic and recycling routes of basolateral proteins at recycling endosomes. Mol Biol Cell. 2007; 18(12):4872–4884. [PubMed: 17881725]
57. Ohno H, Aguilar RC, Yeh D, Taura D, Saito T, Bonifacino JS. The medium subunits of adaptor complexes recognize distinct but overlapping sets of tyrosine-based sorting signals. J Biol Chem. 1998; 273(40):25915–25921. [PubMed: 9748267]
58. Janvier K, Kato Y, Boehm M, Rose JR, Martina JA, Kim B-Y, Venkatesan S, Bonifacino JS. Recognition of dileucine-based sorting signals from HIV-1 Nef and LIMP-II by the AP-1 γ–σ1 and AP-3 δ–σ3 hemicomplexes hemicomplexes. J Cell Biol. 2003; 163(6):1281–1290. [PubMed: 14691137]
59. Doray B, Lee I, Knisely J, Bu G, Kornfeld S. The γ/σ1 and α/σ2 hemicomplexes of cathrin adaptors AP-1 and AP-2 harbor the dileucine recognition site. Mol Biol Cell. 2007; 18(5):1887–1896. [PubMed: 17360967]
60. Mullin JM, McGinn MT. Epidermal growth factor-induced mitogenesis in kidney epithelial cells (LLC-PK1). Cancer Research. 1988; 48:4886–4891. [PubMed: 3261628]
61. Kuwada SK, Lund KA, Li XF, Cliften P, Amsler K, Opresko LK, Wiley HS. Differential signaling and regulation of apical versus basolateral EGF receptors in polarized epithelial cells. Am J Physiol. 1998; 275:C1419–1428. [PubMed: 9843701]
62. Choowongkomon K, Carlin C, Sonnichsen F. A structural model for the membrane-bound form of the juxtamembrane domain of the epidermal growth factor receptor. J Biol Chem. 2005; 280:24043–24052. [PubMed: 15840573]

63. Herzlinger D. Inductive interactions during kidney development. Semin Nephrol. 1995; 15(4):255. [PubMed: 7569405]
64. Matter K, Aijaz S, Tsapara A, Balda MS. Mammalian tight junctions in the regulation of epithelial differentiation and proliferation. Curr Opin Cell Biol. 2005; 17(5):453–458. [PubMed: 16098725]
65. Pieczynski J, Margolis B. Protein complexes that control renal epithelial polarity. Am J Physiol - Renal Physiol. 2011; 300(3):F589–F601. [PubMed: 21228104]
66. Desclozeaux M, Venturato J, Wylie FG, Kay JG, Joseph SR, Le HT, Stow JL. Active Rab11 and functional recycling endosome are required for E-cadherin trafficking and lumen formation during epithelial morphogenesis. Am J Physiol Cell Physiol. 2008; 295(2):C545–556. [PubMed: 18579802]
67. Threadgill DW. Targeted disruption of mouse EGF receptor: effect of genetic background on mutant phenotype. Science. 1995; 269:230–234. [PubMed: 7618084]
68. Sibilia M, Wagner EF. Strain-dependent epithelial defects in mice lacking the EGF receptor. Science. 1995; 269(14):234–238. [PubMed: 7618085]
69. Chen J, Chen J-K, Harris RC. Deletion of the epidermal growth factor receptor in renal proximal tubule epithelial cells delays recovery from acute kidney injury. Kidney Int. 2012; 82(1):45–52. [PubMed: 22418982]
70. Zhang Z, Pascuet E, Hueber P, Chu L, Bichet D, Lee T, Threadgill D, Goodyer P. Targeted inactivation of EGF receptor inhibits renal collecting duct development and function. J Am Soc Nephrol. 2010; 21:573–578. [PubMed: 20133479]
71. Cohen D, Brennwald PJ, Rodriguez-Boulan E, Munsch A. Mammalian PAR-1 determines epithelial lumen polarity by organizing the microtubule cytoskeleton. J Cell Biol. 2004; 164(5): 717–727. [PubMed: 14981097]
72. Waterfield MD, Mayes ELV, Stroobant P, Bennet PLP, Young S, Goodfellow PN, Banting GS, Ozanne B. A monoclonal antibody to the human epidermal growth factor receptor. J Cell Biochem. 1982; 20:149–161. [PubMed: 6188757]
73. Hoffman BL, Takishima K, Rosner MR, Carlin C. Adenovirus and protein kinase C have distinct molecular requirements for regulating epidermal growth factor receptor trafficking. J Cell Physiol. 1993; 157:535–543. [PubMed: 8253865]
74. Yu W, O'Brien LE, Wang F, Bourne H, Mostov KE, Zegers MMP. Hepatocyte growth factor switches orientation of polarity and mode of movement during morphogenesis of multicellular epithelial structures. Mol Biol Cell. 2003; 14(2):748–763. [PubMed: 12589067]
75. Crooks D, Kil SJ, McCaffery JM, Carlin C. E3-13.7 integral membrane proteins encoded by human adenoviruses alter epidermal growth factor receptor trafficking by interacting directly with receptors in early endosomes. Mol Biol Cell. 2000; 11(10):3559–3572. [PubMed: 11029055]
76. Ullrich A, Coussens L, Hayflick JS, Dull TJ, Gray AT, A.W. Lee J, Yardern Y, Libermann TA, Sclessinger J, Downward J, Mayes ELV, Whittle N, Waterfield MD, Seeburg PH. Human epidermal gorwth factor receptor cDNA sequence and aberrant expression of the amplified gene in A431 epidermoid carcinoma cells. Nature. 1984; 309:418–425. [PubMed: 6328312]
77. Avivi A, Lax I, Ullrich A, Schlessinger J, Givol D, Morse B. Comparison of EGF receptor sequences as a guide to study the ligand binding site. Oncogene. 1991; 6:673–676. [PubMed: 2030916]
78. Vagin O, Turdikulova S, Yakubov I, Sachs G. Use of the H,K-ATPase B2 subunit to identify multiple sorting pathways for plasma membrane delivery in polarized cells. J Biol Chem. 2005; 280(15):14741–14754. [PubMed: 15695513]

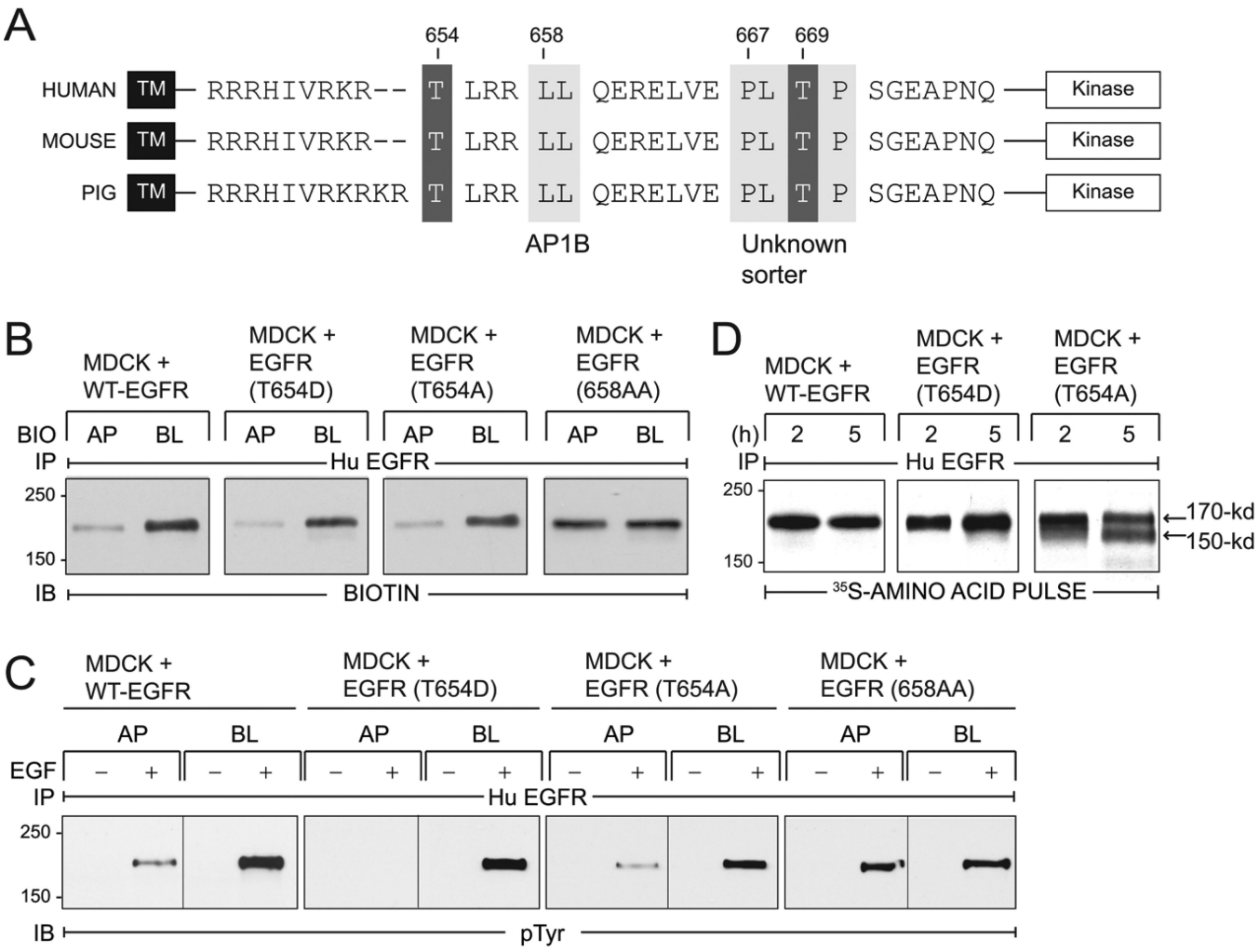

Figure 1. EGFRs with T654A and T654D substitutions localize to BL membranes in established MDCK cell monolayers

(A) EGFR schematic showing transmembrane (TM) and kinase domains with intervening juxtamembrane (JM) amino acid sequence containing known BL sorting signals (light grey boxes): 658-LL that interacts with AP1B (31), and 667-PLTP whose interaction partner is unknown (27). Two known PKC substrates Thr654 and Thr669 are also denoted (dark grey boxes). EGFR JM sequences are highly conserved in human (76), mouse (77), and pig (NCBI Reference Sequence NM_214007.1). (B) Established MDCK cell monolayers with stable expression of human EGFRs listed in the figure were subjected to domain-specific biotinylation. Human EGFR immune complexes were immunoblotted with a biotin-specific antibody. (C) Established MDCK cell monolayers expressing EGFRs were harvested under basal conditions (−) or following a 15-min stimulation with domain-specific EGF (100 ng/ml) (+). Human EGFR immune complexes were immunoblotted with a phosphotyrosine antibody. (D) MDCK cells with human EGFRs were pulse-labeled with ^{35}S-labeled amino acids and harvested after a 2 or 5 h incubation in non-radioactive amino acid chase medium. EGFR immune complexes detected by fluorography.

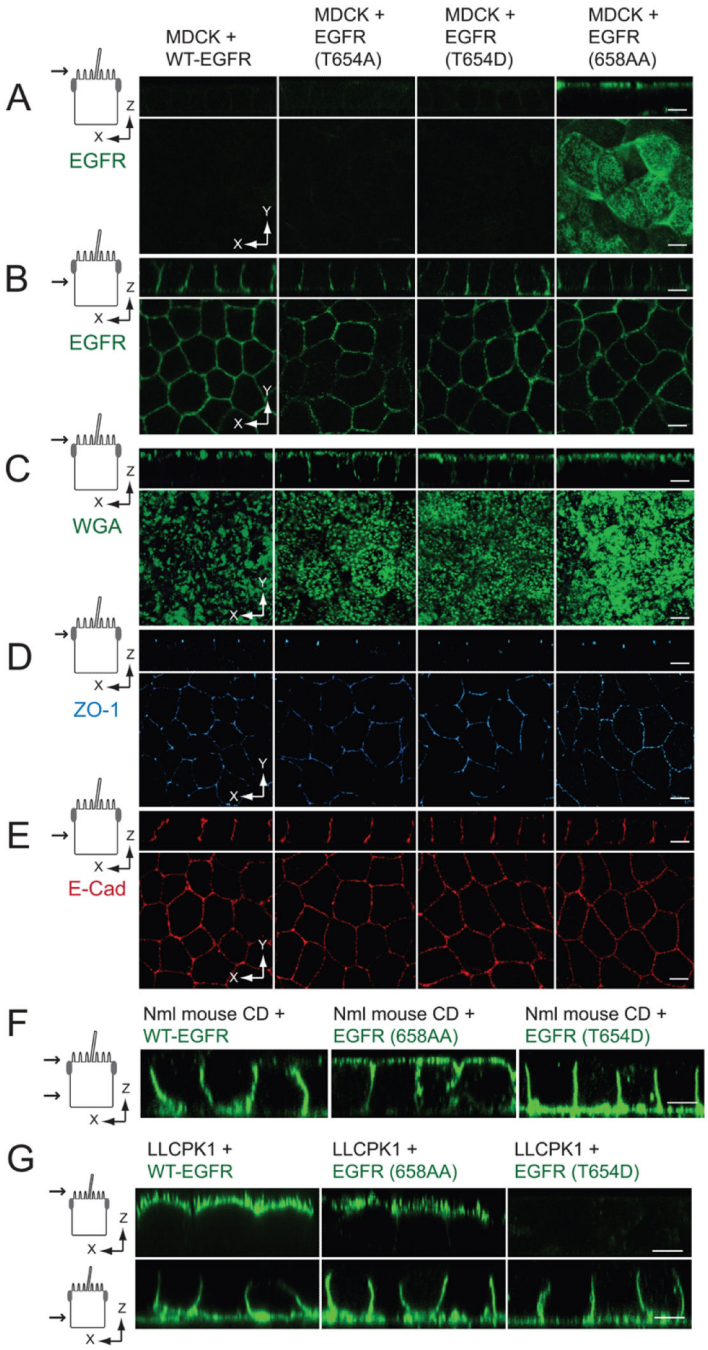

Figure 2. Thr654 regulates EGFR sorting independently of AP1B

(A - B) Vertical *x-z* and horizontal *x-y* confocal sections (see schematics) from fixed MDCK cell monolayers expressing EGFR proteins stained with human-specific EGFR1 antibody (green) added to Ap (A) or BL (B) surface. (C – E) Confocal sections from fixed and permeabilized MDCK cell monolayers stained with Alexa Fluor 488 WGA (green; C) and antibodies to ZO-1 (blue; D) and E-cadherin (red; E). (A-E) Schematics to left show the plane of the vertical confocal image. (F) Confocal images of AP1B positive normal mouse collecting duct (CD) cell monolayers expressing human EGFRs listed in the figure fixed and

stained with EGFR1 (green) added to both surfaces (monolayer leakiness precluded domain-specific EGFR1 staining). (G) Confocal images of AP1B negative LLCPK1 pig epithelial cell monolayers expressing human EGFRs listed in the figure fixed and stained with EGFR1 (green) added to Ap (top) or BL side of the filter. Size bars = 5 μm.

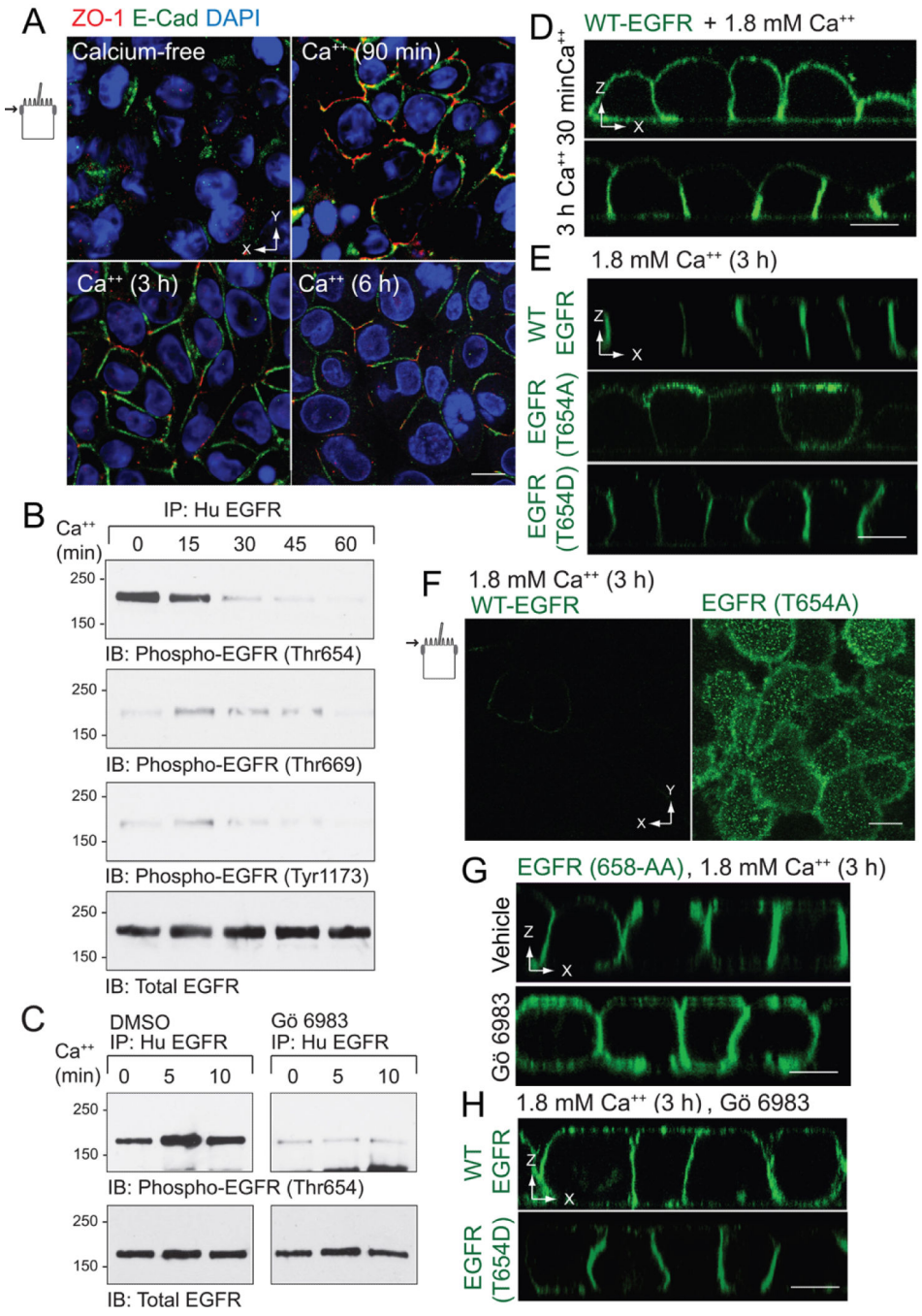

Figure 3. Non-phosphorylatable T654A substitution interferes with BL EGFR polarization in a modified calcium switch model

Contact naïve MDCK cells with WT-EGFR were plated at confluency on permeable filter supports in calcium-free spinner-modification MEM (S-MEM), re-fed with normal MEM containing 1.8 mM Ca^{++} 3 h later, and analyzed at times indicated. (A) Confocal images collected in the plane of the Ap membrane (see schematic) from fixed and permeabilized cells stained with antibodies to ZO-1 (red) and E-cadherin (green) and counterstained with DAPI (blue). (B) Human EGFR immune complexes were immunoblotted with phospho-specific EGFR antibodies listed in the figure and an activation-independent EGFR antibody

to control for protein loading. (C) Same as (B) except cells were pretreated with DMSO vehicle or the broad spectrum PKC inhibitor Gö 6983 (5 μm) during the calcium-free incubation. (D - H) Cells were fixed, permeabilized, and stained with EGFR1 (green) for confocal imaging. Vertical confocal images of MDCK cells with WT-EGFR 90 min or 3 h after the switch to 1.8 mM Ca^{++} (D). Vertical confocal images of MDCK cells with WT-EGFR or EGFRs with Thr654 mutations 3 h after the switch to 1.8 mM Ca^{++} (E). Images collected in plane of the Ap membrane from MDCK cells expressing WT-EGFR or EGFR (T654A) 3 h after the switch to 1.8 mM Ca^{++} (F). Vertical confocal images of MDCK cells expressing EGFR (658-AA) pre-treated with vehicle (top) or Gö 6983 (5 μm; bottom) 3 h after switch to 1.8 mM Ca^{++} (G). Vertical confocal images of MDCK cells with WT-EGFR or EGFR (T654D) pre-treated with Gö 6983 3 h after switch to 1.8 mM Ca^{++} (H). All size bars = 5 μm.

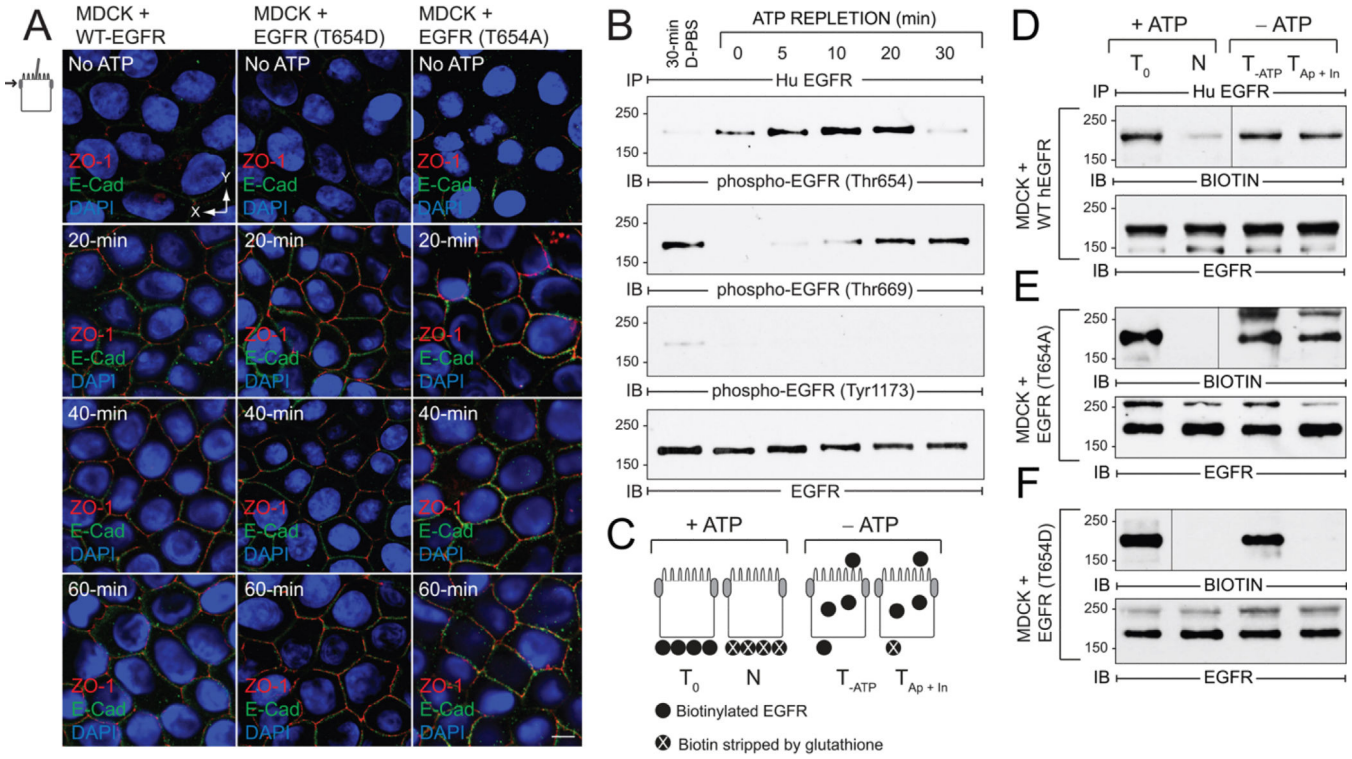

Figure 4. EGFR Thr654 regulates EGFR sorting in ATP depletion-repletion renal injury model

ATP was depleted by incubating mature MDCK monolayers in PBS supplemented with 2-deoxy-d-glucose and antimycin A for 30 min, and then replenished by re-feeding cells with complete media for times indicated in the figure. (A) Confocal images from just beneath the Ap membrane in cells stained with antibodies to ZO-1 (red) and E-cadherin (green) and counterstained with DAPI (blue). Size bar = 5 μm. (B) Cells were lysed to recover human EGFR immune complexes for immunoblotting with phospho-specific EGFR antibodies listed in the figure and an activation-independent EGFR antibody. Control cells were incubated in Dulbecco's PBS (D-PBS) for 30 min without ATP depletion. (C) Schematic showing experimental procedure for evaluating BL EGFR distribution in ATP-depleted cells. Established MDCK cell monolayers were labeled from the BL side with a cleavable biotin reagent. T_0, total biotinylated EGFR (positive control); N, biotin stripped from BL side immediately after biotinylation (negative control); T_{-ATP}, total biotinylated EGFR from ATP-depleted cells (control for stability of biotinylated EGFR); $T_{Ap + In}$, biotin stripped from BL surface in ATP-depleted cells (internalized biotinylated EGFR and biotinylated EGFR reinserted in Ap membrane). (D - F) Cells expressing WT-EGFR (D), EGFR (T654A) (E), or EGFR (T654D) (F) were treated according to the scheme in (C). EGFR immune complexes were resolved by non-reducing SDS-PAGE for immunoblotting with a biotin antibody (top panels) or an EGFR antibody to control for protein loading (bottom panels). Representative immunoblots from at least two independent experiments.

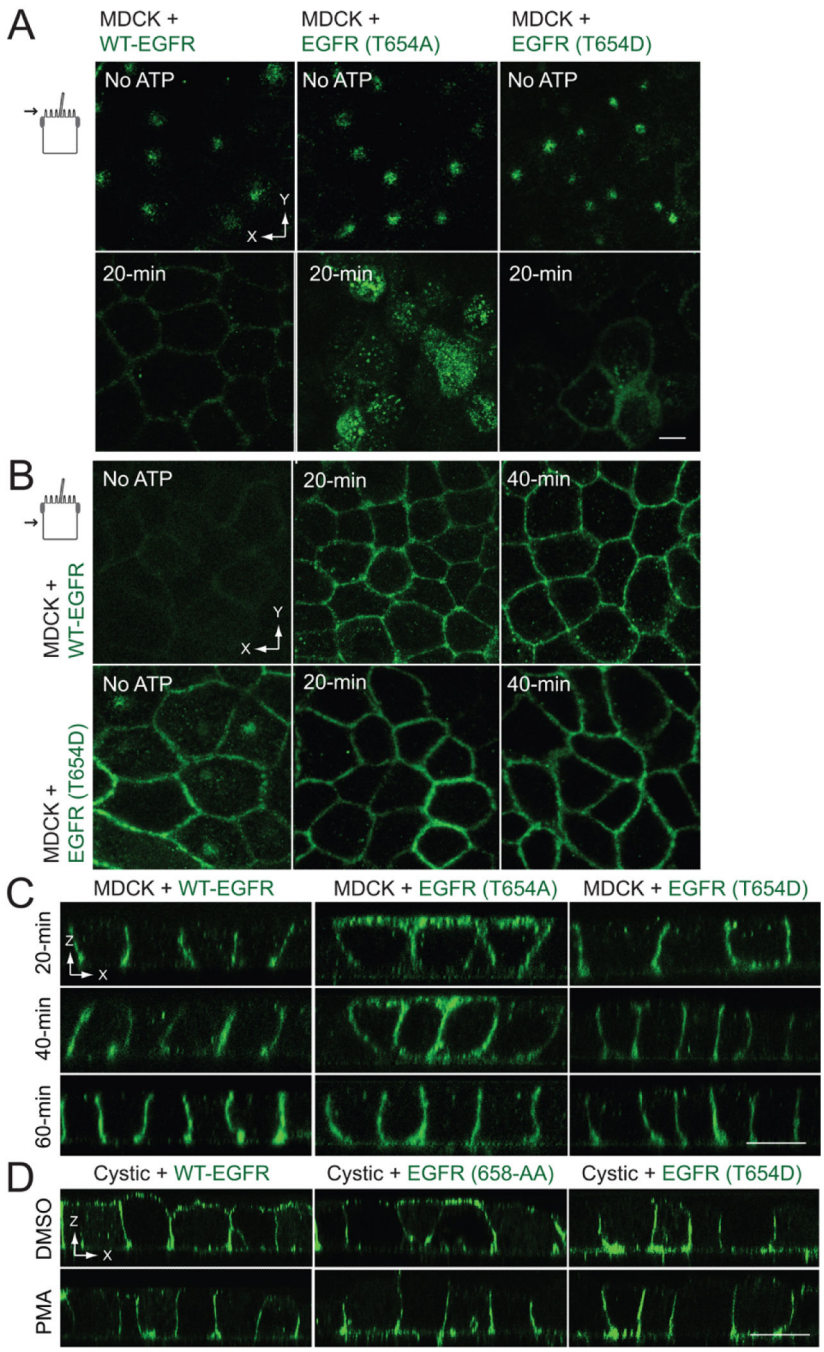

Figure 5. Thr654 regulates BL EGFR delivery in an ATP depletion-repletion renal injury model

ATP depletion-repletion experiments were carried out exactly as described in Figure 4. (A and B) Horizontal confocal images taken in the plane of the Ap membrane (A) or the middle of the lateral membrane (B) from fixed cells stained with EGFR1 (green) at the end of the 30-min ATP depletion period before ATP repletion (top panels) or following a 20-min incubation in complete media to replenish ATP (bottom panels). (C) Vertical confocal images images from fixed cells stained with EGFR1 (green) at times indicated during the ATP repletion period. (D) Cystic cells derived from the BPK model for ARPKD with stable

EGFR expression were incubated with DMSO vehicle or PMA (1 μm) for 30 min, stained with EGFR1 (green) without permeabilization, and analyzed by confocal microscopy. All size bars = 5 μm.

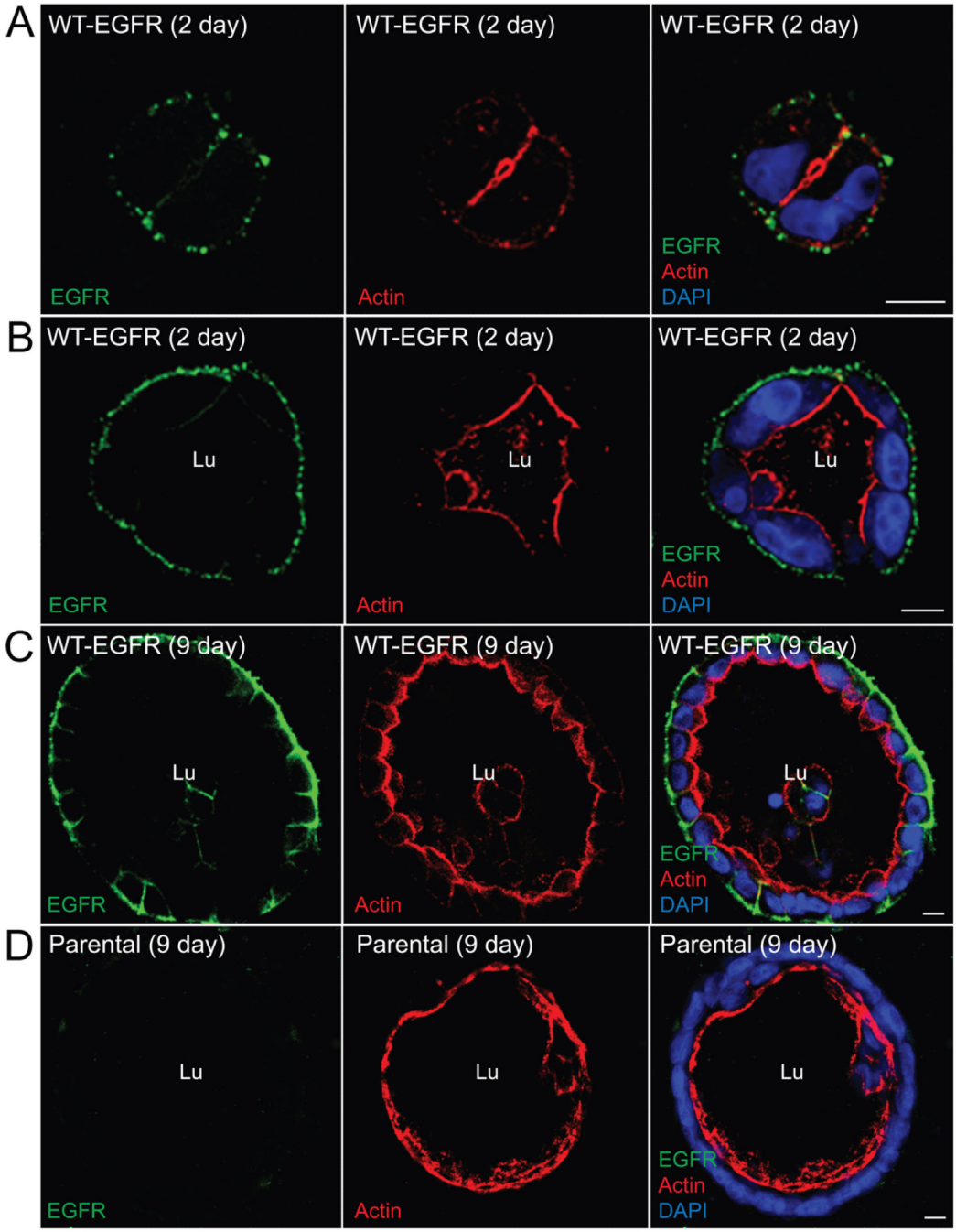

Figure 6. WT-EGFR expression supports normal cyst morphology in 3D collagen gels

A stable MDCK cell line expressing WT-EGFR (A - C) and parental MDCK cells with physiological levels of endogenous canine EGFR (D) were grown in collagen gels for 2 (A, B) or 9 (C, D) days. Gels were digested with collagenase to increase the accessibility of antibodies to cysts, fixed after permeabilization with β-escin, and stained with EGFR1 antibody (green) and phalloidan (red) and DAPI (blue) to visualize actin and nuclei, respectively, for confocal imaging. Size bars = 10 μm. Lu = lumen.

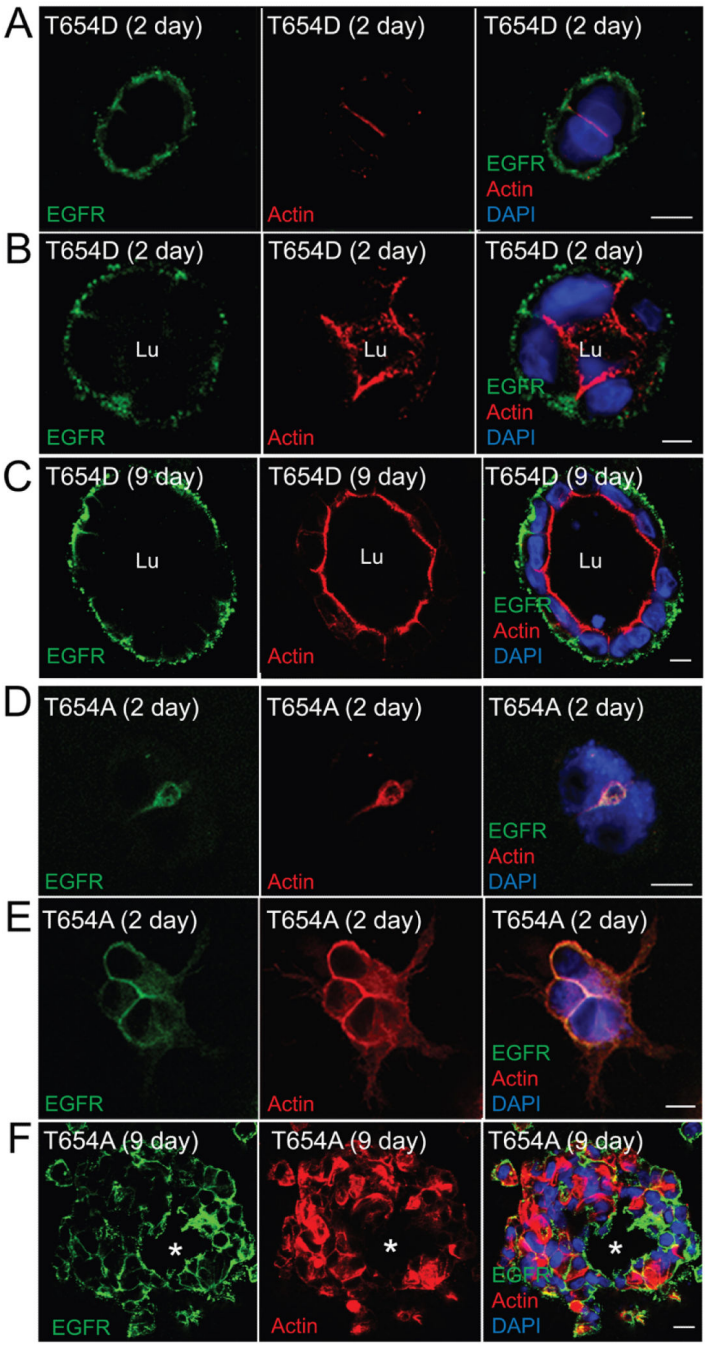

Figure 7. Thr654 regulates cell adhesion in 3D collagen gels

Cells expressing EGFR (T654D) (A – C) or EGFR (T654A) (D –F) were propagated in collagen gels for 2 (A, B, D, E) or 9 (C, F) days and analyzed exactly as described in the legend to Fig. 6. Asterisks in F indicate rudimentary lumen. Size bars = 10 μm.

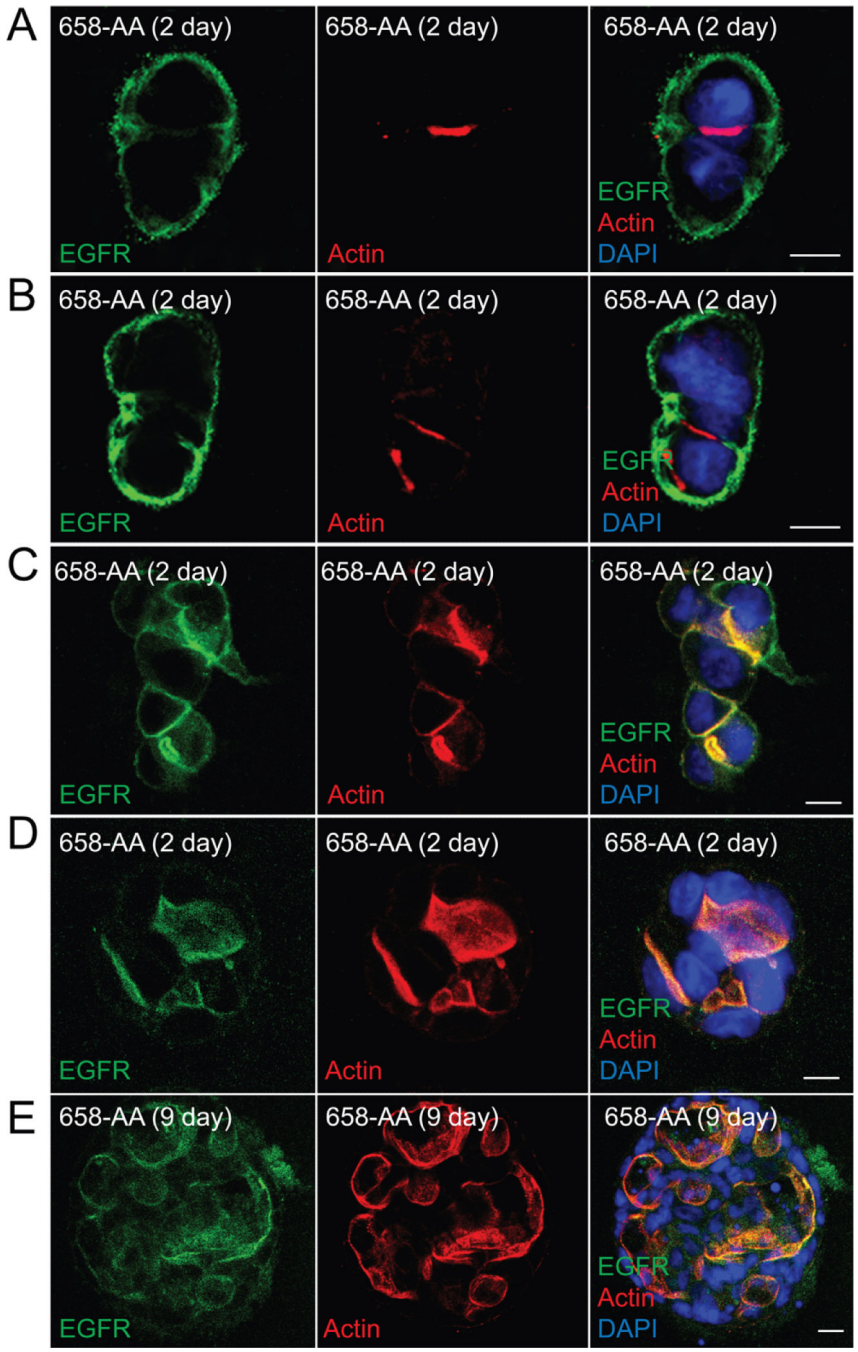

Figure 8. AP1B-dependent EGFR sorting regulates lumen formation in 3D collagen gels

Cells expressing AP1B defective EGFR (658-AA) were propagated in collagen gels for 2 (A - D) or 9 (E) days and analyzed exactly as described in the legend to Fig. 6. Size bars = 10 μm.

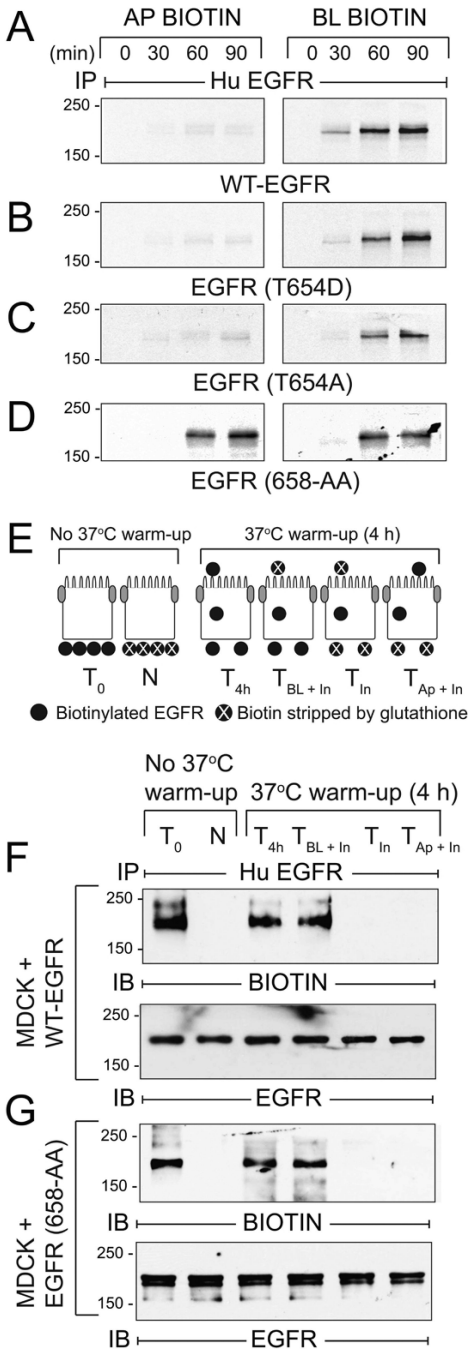

Figure 9. AP1B regulates BL EGFR membrane delivery in the biosynthetic route in established MDCK cell monolayers

(A - D) AP1B-positive epithelial cells expressing human EGFRs listed in the figure were pulse-labeled with ^{35}S-labeled amino acids and biotinylated at Ap or BL surface at times indicated during non-radioactive amino acid chase. EGFR immune complexes were purified using streptavidin beads for SDS-PAGE and fluorography. (E) Schematic showing experimental procedure for evaluating BL-to-Ap EGFR transcytosis [adapted from (78)]. Established MDCK cell monolayers were biotinylated from the BL side. T_0, total biotinylated EGFR (positive control); N, biotin stripped immediately after biotinylation from

BL side (negative control); T_{4h}, total biotinylated EGFR from cells incubated at 37°C for 4 h (control for stability of biotinylated EGFR); $T_{BL + In}$, biotin stripped from Ap surface after 4 h 37°C incubation (internalized biotinylated EGFR and biotinylated EGFR remaining on BL membrane); T_{In}, biotin stripped from both surfaces after 4 h 37°C incubation (internalized biotinylated EGFR); $T_{Ap + In}$, biotin stripped from BL surface after 4 h 37°C incubation (internalized biotinylated EGFR and biotinylated EGFR transcytosed to Ap membrane). (F - G) MDCK cells expressing WT-EGFR (F) or EGFR (658-AA) (G) treated according to the scheme in (E) were lysed and human EGFR immune complexes were resolved by non-reducing SDS-PAGE for immunoblotting with a biotin antibody (top panels), or an EGFR antibody to control for protein loading (bottom panels). Representative immunoblots from at least two independent experiments.

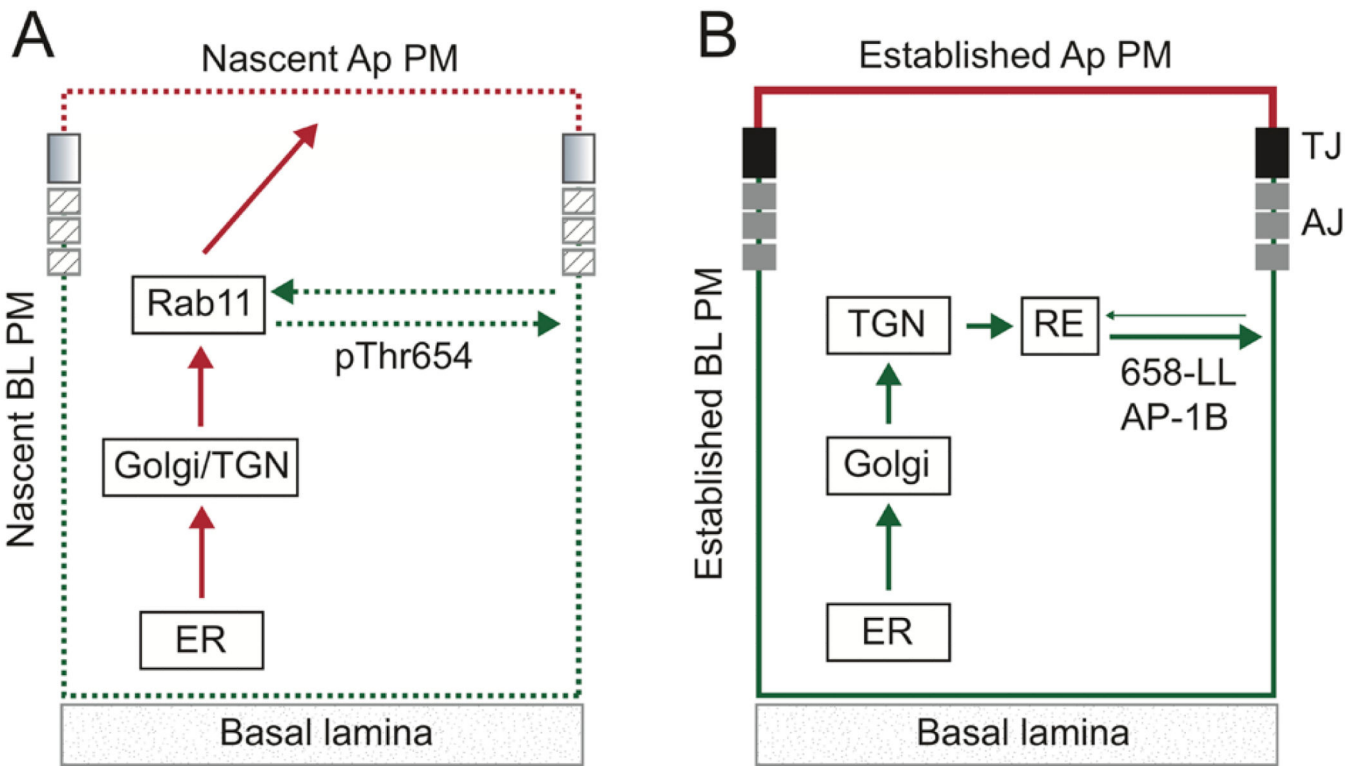

Figure 10. Summary model

Schematics depicting putative EGFR sorting pathways employed during cell-cell junction assembly (A) and in established epithelial cell layers (B). (A) PKC-dependent Thr654 phosphorylation activates a latent BL sorting signal during formation of new cell-cell junctional complexes (shaded and hatched boxes). The sorting route presumably involves $Rab11^+$ recycling endosomes based on our previous results that EGFR (T654D) co-localizes with $Rab11^+$ in MDCK cells (31). Data in this manuscript suggest the latent signal regulates recycling and retention on nascent BL membranes (dashed green). The latent signal may also divert EGFRs *en route* to the Ap membrane *via* a previously characterized N-glycan-dependent biosynthetic route (red) (29). (B) We have also shown previously that BL EGFR localization is regulated by interactions between a dileucine motif 658-LL and epithelial cell specific clathrin adaptor AP1B in cells with established cell-cell TJ and AJ (solid black and grey boxes) (31). Data presented in this manuscript indicate AP1B sorts EGFRs in a biosynthetic pathway most likely *via* post-TGN endosome sorting intermediates (solid green). We cannot exclude the possibility AP1B also regulates BL EGFR recycling under basal conditions. AJ: *adherens* junction; RE: recycling endosome; ER: endoplasmic reticulum; TGN: *trans*-Golgi network; TJ: tight junction.